Accepted to *Ecological Informatics*, 25 Oct 2022

TITLE: Spatial-temporal interpolation of satellite geomagnetic data to study long-distance animal migration

AUTHORS:

Aranya Iyer[1*]

Fernando Benitez-Paez[2,3]

Vanessa Brum-Bastos[2,4,5]

Ciarán D. Beggan[6]

Urška Demšar[2]

Jed A. Long[1,2]

Affiliations:

[1] Department of Geography and Environment, Western University, 1151 Richmond St, London, Ontario N6A 3K7, Canada

[2] School of Geography and Sustainable Development, Irvine Building, University of St Andrews, North Street, St Andrews, KY16 9AL, Scotland, UK

[3]The Alan Turing Institute, British Library, 2QR, John Dodson House, 96 Euston Rd, London NW1 2DB, United Kingdom

[4] Institute of Geodesy and Geoinformatics, Wroclaw University of Environmental and Life Sciences, Norwida 25, 50-375 Wrocław, Poland

[5] School of Earth and Environment, University of Canterbury, 20 Kirkwood Avenue, Upper Riccarton, Christchurch 8041, New Zealand

[6]British Geological Survey, Research Ave South, Riccarton, Edinburgh, EH14 4AP, Scotland, UK

***Corresponding author:** aiyer25@uwo.ca

Present address:

Department of Geography and Environment

Social Science Centre Rm 2322, Western University

London, Ontario, Canada

N6A 5C2

Abstract

Introduction: Increased access to remote sensing datasets presents opportunities to model an animal's in-situ experience of the landscape to study behavior and test hypotheses such as geomagnetic map navigation. MagGeo is an open-source tool that combines high spatiotemporal resolution geomagnetic data with animal tracking data. Unlike gridded remote sensing data, satellite geomagnetic data are point-based measurements of the magnetic field at the location of each satellite. MagGeo converts these measurements into geomagnetic values at an animal's location and time. The objective of this paper is to evaluate different interpolation methods and data frameworks within the MagGeo software and quantify how accurately MagGeo can model geomagnetic values and patterns as experienced by animals.

Method: We tested MagGeo outputs against data from 109 terrestrial geomagnetic observatories across 7 years. Unlike satellite data, ground-based data are more likely to represent how animals near the Earth's surface experience geomagnetic field dynamics. Within the MagGeo framework, we compared an inverse-distance weighting interpolation with three different nearest-neighbor interpolation methods. We also compared model geomagnetic data with combined model and satellite data in their ability to capture geomagnetic fluctuations. Finally, we fit a linear mixed-effect model to understand how error is influenced by factors like geomagnetic activity and distance in space and time between satellite and point of interest.

Results and conclusions: The overall absolute difference between MagGeo outputs and observatory values was less than 1% of the total possible range of values for geomagnetic components. Satellite data measurements closest in time to the point of interest consistently had lowest error which likely reflects the ability of the nearest neighbour in time interpolation method to capture small continuous daily fluctuations and larger discrete events like geomagnetic storms.

Combined model and satellite data also capture geomagnetic fluctuations better than model data alone across most geomagnetic activity levels. Our linear mixed-effect models suggest that most of the variation in error can be explained by location-specific effects originating largely from local crustal biases, and that high geomagnetic activity usually predicts higher error though ultimately remaining within the 1% error range. Our results indicate that MagGeo can help researchers explore how animals may use the geomagnetic field to navigate long distances by providing access to data and methods that accurately model how animals moving near the Earth's surface experience the geomagnetic field.

Keywords:

Geomagnetism, navigation cues, animal movement, wildlife tracking, Swarm constellation, CHAOS-7 model

1. Introduction and background

1.1 Introduction

Understanding how migratory animals navigate the landscape is challenging not least because of the spatiotemporal range of some migrations (Wilcove & Wikelski, 2008). Access to remote sensing imagery has influenced our understanding of how and why an animal interacts with its environment (Pettorelli et al., 2014). However, the predominant use of optical remote sensing imagery often restrains how we model an animal's relationship to its surroundings. Remote sensing satellites with sensors, such as Synthetic Aperture Radars (SARs) and Light Detection and Ranging (LiDAR), offer opportunities for novel lines of questioning in wildlife movement ecology. Satellites with geophysical sensors measuring the Earth's magnetic field are an example of an underexplored non-optical resource that can bring new insights, especially with regards to the magnetic map hypothesis (Lohmann et al., 2007; Mouritsen, 2014; Naisbett-Jones et al., 2017; Wiltschko & Wiltschko, 2013).

The geomagnetic field is an invisible shield around the Earth that protects the planet from incoming solar particles (Campbell, 2003). Large scale geomagnetic patterns vary predictably across space and time, thus allowing human navigators to reliably use geomagnetic information for wayfaring for many centuries. Animals who are capable of sensing and perceiving the geomagnetic field may also use geomagnetic patterns to make navigation decisions during migration (Lohmann et al., 2007; Mouritsen & Heyers, 2016; Wiltschko & Wiltschko, 2021). The underlying mechanisms of the geomagnetic navigation strategies vary between species and are highly debated in the literature (Åkesson et al., 2005; Holland et al., 2009; Muheim et al., 2018; Pollonara et al., 2015). Specifically, migratory navigation consists of two tasks: 1) knowing the current location (geographic positioning) and 2) knowing in which direction to go (compass orientation). Some research suggests that animals use geomagnetic information for orientation, and it is also possible that animals use two or more geomagnetic values to build cognitive maps for positioning (although this has not been proven and is at present still debated) (Mouritsen, 2018; Sokolovskis et al., 2018; Wikelski et al., 2015). Physiological capabilities to sense geomagnetic values have been tested in laboratory experiments, alongside physical or virtual displacement that demonstrate how a bird's migratory direction oscillates with changes in a magnetic environment (Kishkinev, 2015). The exact sensitivity range to changes in absolute geomagnetic values is unclear and likely varies by species, internal states, and external conditions. Some experiments suggest ranges from 15 nT to 200 nT for total intensity (Beason & Semm, 1987; Semm & Beason, 1990), 2° to 5° for inclination (Schwarze et al., 2016), and at least 8° for declination sensitivity (Chernetsov et al., 2017). There are even fewer experiments that have explored how wild migrants respond to the geomagnetic field during the actual migration and what strategies they use for orientation and positioning. To understand what happens outside of controlled laboratory settings, there has been a push to test geomagnetic strategies from a data-driven, geospatial perspective by taking advantage of open-source geomagnetic models and satellite data (Zein et al., 2021, 2022).

To look at this, previous studies have successfully combined geomagnetic model estimates with animal tracking data (Åkesson & Bianco, 2016, 2017; Sokolovskis et al., 2018; Zein et al., 2021). Model estimates are typically geomagnetic field values predicted using a set of model coefficients that are informed by satellite geomagnetic data collected during periods of low geomagnetic activity otherwise known as quiet-time (Chulliat et al., 2015; Matzka et al., 2010; Olsen et al., 2006). Model estimates are continuous across time allowing daily estimates for any latitude, longitude, and altitude combination (location in 3D space). As such, estimates are useful for movement ecologists trying to understand how geomagnetic information can influence animal behavior across the entire migratory trajectory. For example, Åkesson & Bianco (2016, 2017) used the 11th Generation International Geomagnetic Reference Field (IGRF-11) model to create simulated migratory paths built from model estimates. They compared these trajectories with observed paths recorded by migratory birds carrying GPS trackers. Zein et al. (2021) used IGRF-12 to combine migratory bird tracks with model estimates to test different geomagnetic navigation strategies. Studies concluded that a geomagnetic compass mechanism is possible though further exploration about an animal's response to actual geomagnetic conditions during migration was restricted due to data limitations (Zein et al., 2022).

Model estimates capture much of the variability in the geomagnetic field, but not all and especially not the dynamics that may affect an animals' instantaneous responses to the contemporaneous geomagnetic conditions. The geomagnetic field varies across space and time at different scales. Across space, there are both large planetary variations of the field generated by Earth's core and small-scale changes related to crustal field generated by magnetic rocks in the Earth's crust. Temporally, the crustal field changes slowly over millions of years, while the core field changes over years to decades – this is called secular variation. However, the field also changes over the course of the day in response to the variable solar wind, which generates fluctuations in the ionosphere and magnetosphere (Courtillot & Le Mouel, 1988). Solar storms and large solar flares can further lead to disturbances over much shorter temporal scales (seconds to hours) known as geomagnetic storms, whose effects can range from benign and beautiful auroral light displays to technological disruptions, such as satellite anomalies and power blackouts (Babayev et al., 2006; Hapgood, 2012; Kikuchi, 2003; Lanza & Meloni, 2006). Specifically, model estimates omit fine-scale spatial variability created by very local but acute geomagnetic anomalies in the crustal field, and they also do not represent the short-term temporal dynamics of the field, as the models are derived from data largely measured during quiet-time conditions. This means that model estimates do not wholly represent the geomagnetic landscape as experienced by animals (Beggan, 2022; Benitez-Paez et al., 2021; Bianco et al., 2019; Krylov, 2017; Zein et al., 2021).

Raw geomagnetic data collected continuously by sensors on-board satellites are a source of localized higher spatial and temporal resolution geomagnetic information. The most comprehensive example is the European Space Agency's (ESA) recent mission of Swarm satellites (European Space Agency, 2020; Friis-Christensen et al., 2006; Olsen et al., 2013). Since 2014, two satellites in near-polar parallel circular orbits and a third in a drifting local time circular orbit, are continuously collecting data as they move over the Earth's surface at an altitude of 450-510 km (Friis-Christensen et al., 2006, 2008). Unlike model estimates, satellites measure the actual magnetic conditions, which include contributions from all major magnetic sources (core, crust, ionosphere) as well as the real-time effects of the interaction with the solar wind. Swarm data are openly available through the VirES interface (European Space Agency, 2021; Kloss, 2021).

MagGeo is an open-source tool that takes advantage of the high resolution of Swarm data and combines it with model estimates to create an accurate representation of magnetic conditions at a specific location and moment in time (Benitez-Paez et al., 2021), thus enabling linkage of satellite geomagnetic data with animal tracking data (for example, trajectories collected by GPS tags). MagGeo gets model estimates from the 7th Generation of the CHAMP, Ørsted and SAC-C (CHAOS-7) model of the Earth's magnetic field (Finlay et al., 2020). A major challenge when combining animal tracking data with environmental variables like geomagnetic data is matching the spatial and temporal resolution of different datasets (Brum-Bastos et al., 2021). Interpolation methods are required to overcome these differences because it is rare that a measured environmental variable and a moving animal coincide perfectly in space and time. After correcting for the difference in altitudes between satellite orbits and animals moving near the Earth's surface, MagGeo uses an inverse-distance weighting interpolation method to combine Swarm satellite data with GPS tracking data to allow movement ecologists to test hypotheses about geomagnetism and animal movement from a geospatial data-driven perspective.

Benitez-Paez et al. (2021) performed an initial error and accuracy analysis of MagGeo though, it was limited to three test locations in Europe for six days of variable geomagnetic activity. A more thorough error and accuracy analysis is required to ensure MagGeo's useability for locations outside of Europe and across various time periods. Furthermore, MagGeo assumes that (1) inverse-distance weighting and (2) a combination of model estimates and satellite data are the most likely interpolation method and data structure to accurately model the geomagnetic field as experienced by animals. These assumptions have not been tested.

We perform a global error and accuracy analysis for MagGeo by testing more than 100 locations across 7 years (2014-2020) and following common practices outlined by the geophysical community (Beggan, 2022; Chulliat et al., 2015; Macmillan & Olsen, 2013). We evaluate accuracy measures across four spatiotemporal interpolation methods: (1) inverse-distance weighting, and three nearest-neighbor methods for (2) space, (3) time and (4) spacetime. Next, we compare the accuracy between model estimates (from CHAOS-7) and fused model estimate and satellite data (combining CHAOS-7 and Swarm satellite data). We highlight important considerations for researchers hoping to model the geomagnetic field through MagGeo to ask questions about animal navigation. We also demonstrate the benefits of performing error and accuracy assessments of remotely sensed environmental data that are applicable to movement ecologists. We believe that studies like ours encourage cross-disciplinary collaboration and will become increasingly important with the current trends in technology evolution and data accessibility (Guilford et al., 2011; Kays et al., 2022; Nathan et al., 2022).

1.2 Background

1.2.1 Earth's geomagnetic field

The Earth's magnetic field is notionally like a bar magnet with field lines exiting the geomagnetic south pole (near Antarctica) and entering the geomagnetic north pole (presently within Ellesmere Island). In detail, the geomagnetic field is far more complex and has various components apart from polarity (Figure 1A). Total field intensity (F) and the horizontal component of the field intensity (H) are two scalar quantities that measure the magnitude of the geomagnetic field vector in nanoteslas (nT). Inclination (I) and declination (D) are angular components of the geomagnetic field vector measured in degrees. Inclination refers to the angle between the field vector and the Earth's horizon whereas declination is the angle between magnetic north and the geographic north pole. Declination is used to align the geomagnetic field on the Earth and is not a natural property of the field since it requires additional knowledge of the relative position of the geographic North and South poles. Geometrically, these components (FHID) can be calculated from values collected by geomagnetic sensors which are measured in the North (N), east (E) and center (C) cartesian coordinate system (Figure 1A) (Campbell, 2003). There are multiple sources of Earth's geomagnetic field, the principal being the geodynamo in the liquid outer core which accounts for around 98% of the total field and has a surface strength of between 23000-60000 nT. Next, the magnetic minerals in the local subsurface (curst) varies between 10-1000 nT depending on location. Electrical currents in the ionosphere at approximately 100-1000 km above the Earth's surface and electrical currents in the magnetosphere which extends even further into outer space are the two final sources of the geomagnetic field (Figure 1B). Different altitudes at the same geographic coordinate will have different geomagnetic values depending on the proximity to the geomagnetic sources (Campbell, 2003; Hulot et al., 2010; Thébault et al., 2010). The typical strength of the external field in magnetically quiet conditions is 20-50 nT but rises to >1000 nT in active periods. Geomagnetic field activity is quantified on a quasi-logarithmic scale called the Kp index (with values of 0-9) which often accompanies open-source geomagnetic data (Matzka et al., 2021). During periods of high solar activity such as geomagnetic storms, values of the geomagnetic field can change rapidly particularly at the mid to high latitudes.

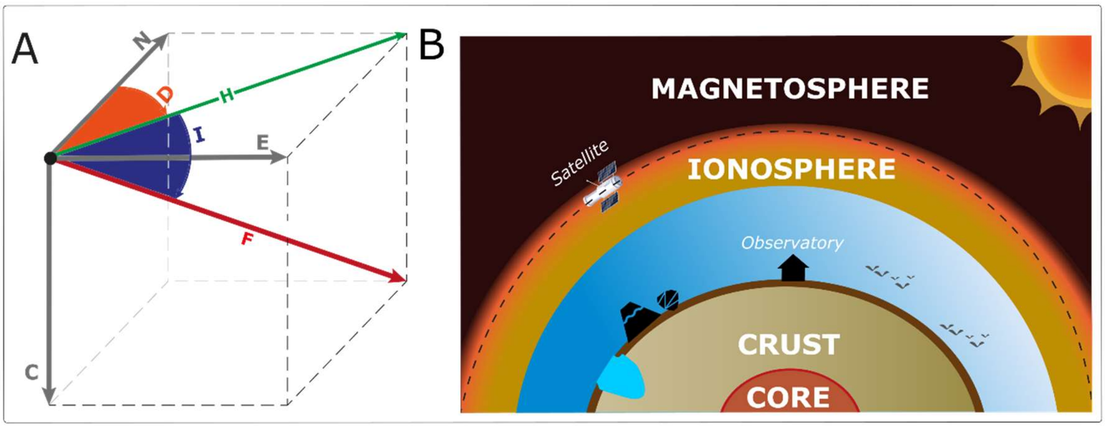

Figure 1. The main components of the geomagnetic field. **A.** The geomagnetic coordinate system is in the North-East-Centre (NEC) coordinate frame shown in gray with the 4 geomagnetic components highlighted in color: declination (D) in orange, inclination (I) in blue, horizontal intensity (H) in green, and total intensity (F) in red. **B.** The 4 main contributors to the geomagnetic field from innermost to outermost: core, crust, ionosphere, and magnetosphere. Examples of geomagnetic anomalies due to lithosphere composition represented by symbols for water body, volcano, and exposed magnetic rock. Satellite orbiting in the ionosphere and the geomagnetic observatory are representations for the two main geomagnetic data sources.

1.2.2 Geomagnetic data sources

Geomagnetic data are traditionally collected at ground-based observatories. The INTERMAGNET network of observatories (Figure 2) currently has 126 operational stations across the world that collect geomagnetic data (INTERMAGNET, 2020) available at second-, minute- and hour cadences. Since observatories are located at ground level, their data are heavily influenced by the core and crustal components of the geomagnetic field (Thébault et al., 2010).

While they have high temporal resolution, data from INTERMAGNET observatories are limited to their locations which are irregularly distributed. For example, there are only six stations in Africa and six stations in South America. The low station density impairs study of long-distance animal migration that can span multiple continents.

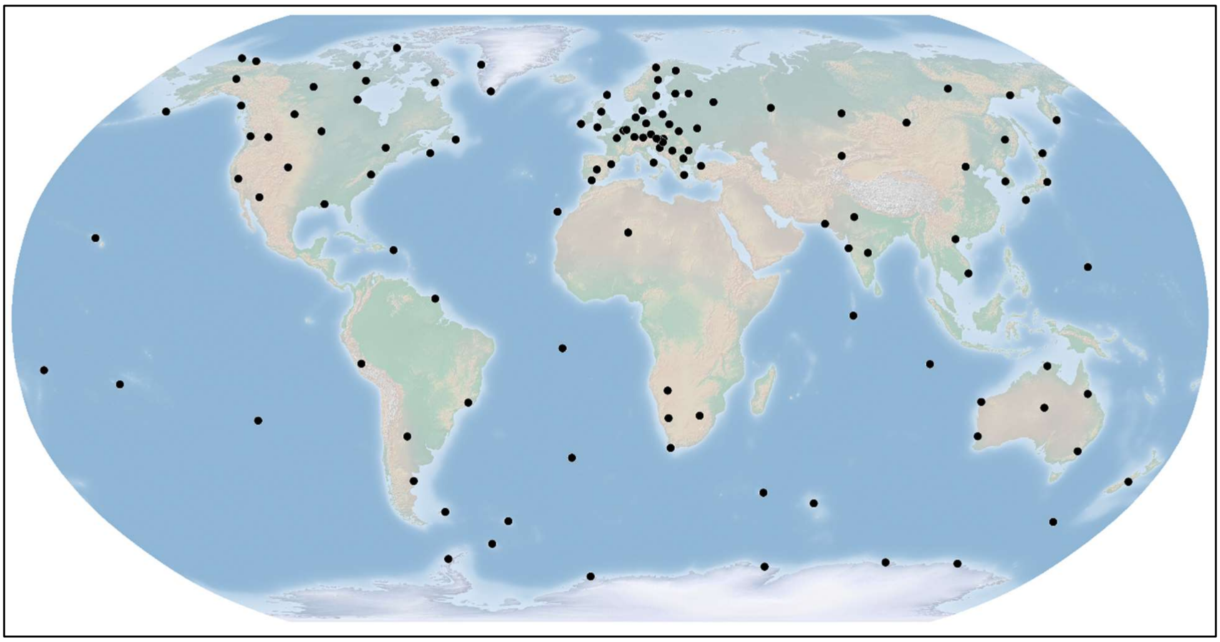

Figure 2. Global distribution of INTERMAGNET observatories (n=126).

In contrast to ground stations, polar-orbiting satellites with on-board magnetometers collect globally distributed data on the geomagnetic field for locations on their orbit. These satellites collect data at high altitudes (400-500 km) and are strongly influenced by the ionosphere (Benitez-Paez et al., 2021; Campbell, 2003) (Figure 1B). An ongoing mission to gather satellite geomagnetic data is operated by ESA with their launch of three Swarm satellites in late-2013 (Friis-Christensen et al., 2006; Olsen et al., 2013). One-second resolution data from these satellites are available within 96 hours of collection and can be accessed through the VirES platform (European Space Agency, 2021).

A combination of observatory data, satellite data, and ground data are used to inform creation of geomagnetic models which are often spherical harmonic models determined by a set of so-called Gauss coefficients (Chulliat et al., 2015; Olsen et al., 2006; Sabaka et al., 2020). Geomagnetic values are then estimated from these model coefficients and are used for geophysical studies, long-term monitoring, resource exploration and extraction, and are updated periodically to account for the non-linear continuous changes in the geomagnetic field (secular variation). Due to the ease at which model estimates can be computed for each unique location in 3D space, they are often used in non-geophysical field applications, and have previously been used in the analysis of animal migrations (Boström et al., 2012; Komolkin et al., 2017). Due to the complexity of the field, model estimates alone however cannot capture the spatial and temporal variability outside of quiet-time and at the scale that animals moving near the Earth's surface might experience the geomagnetic field.

2. Data and Methods

MagGeo is an open-source tool that combines model estimates and satellite data and attaches it to wildlife tracking data anywhere on the Earth's surface from November 2013 to present. Model estimates are available for any 3-D location and timestamp of an animal tracking fix. MagGeo uses the CHAOS-7 model to estimate the core, crustal and magnetosphere contributions of the geomagnetic field (Figure 1B). CHAOS-7 model estimates do not calculate ionospheric contributions. There are other models, such as the Swarm Comprehensive models (Sabaka et al., 2020), which provide estimates for the ionosphere. The flexibility of the MagGeo framework can allow for replacing the CHAOS-7 values with other data sources that provide complete model estimates of the geomagnetic field based on user preference and research objectives. Model estimates however will include only averaged quiet time values for the ionosphere and subsequently will not capture the local, real-time variation. We include the Swam satellite data to introduce this local and temporal variability to CHAOS-7 model estimates.

For the CHAOS-7 model, the contributions from the core, lithosphere and magnetosphere are added to create an estimate of geomagnetic values at the ground level:

$$CH_g = CH_g^C + CH_g^L + CH_g^M \qquad [1]$$

Where CH represents the CHAOS-7 model estimates, the subscript g represents geomagnetic estimates at ground level altitude and the superscripts represent the different geomagnetic source components (C = core, L = lithosphere, M = magnetosphere). As the model estimates are designed to be continuous, they do not require spatial interpolation.

Raw geomagnetic data collected by satellites from ESA's Swarm constellation (European Space Agency, 2021; Friis-Christensen et al., 2006) are also freely available. It is unlikely however that geomagnetic values at satellite altitude will represent the geomagnetic field as experienced by an animal at the ground level. To correct for this altitude difference, we calculate satellite residuals by subtracting CHAOS-7 model estimates at satellite altitude for the core, lithosphere, and magnetosphere contributions.

$$SW_s^{Res} = SW_s - CH_s^C - CH_s^L - CH_s^M \quad [2]$$

Where SW represents raw geomagnetic data collected by Swarm satellites, the subscript s represents values collected or estimated at satellite altitude and the superscripts represent the different geomagnetic source components (C, L, or M) or the satellite residuals (Res). The Swarm satellite residuals (SW_s^{Res}) primarily represent ionosphere contributions at satellite altitude though they are ultimately a combination of ionosphere, magnetosphere, crust, and other smaller influences on the geomagnetic field. SW_s^{Res} introduces temporal variability with fine resolution to capture the dynamic nature of the geomagnetic field outside of quiet-time values as estimated by geomagnetic models.

Given the satellite orbit however, it is unlikely that the satellite will be directly above a location on Earth for a specific timestamp. Therefore, geomagnetic data collected by satellites require interpolation to attach to an animal tracking fix. SW_s^{Res} can be interpolated to the animal tracking point by creating a space-time kernel. This kernel is a space-time cylinder where the radius of the cylinder has spatial dimensions, and the height has a temporal dimension (Figure 3A). Based on the Swarm satellites' polar orbits, the kernel's spatial boundary (the size of the cylinder's base, R in Figure 3A) varies with latitude, with smaller spatial boundaries at higher latitudes (approximately 900 km) compared to equatorial latitudes (approximately 1800 km). The kernel's temporal boundary (the height of the cylinder) is +/- 4 hours (ΔT) from the tracking fix, again based on the properties of the polar orbit and to ensure that sufficient satellite data are present at lower latitudes (Benitez-Paez et al., 2021).

SW_s^{Res} within the space-time kernel are then linked to the animal tracking fix using a spatiotemporal interpolation method (Figure 3B). Benitez-Paez et al. (2021) proposed inverse distance weighting (IDW) where the space-time distance (dST) is calculated to account for both the distance in space (measured in km; dS) and time (measured in seconds; dT) between the satellite residual and the tracking fix. Data points closest in space-time distance (lowest dST) are weighted higher than those farther away and the sum of all weights in each spacetime kernel is 1. We propose three alternative nearest neighbour methods that are both simpler, and potentially more accurate for spatiotemporal interpolation of satellite residuals to wildlife tracking fixes.

The nearest neighbour in space (NNS) interpolation method uses the residuals from the satellite data point closest in space (lowest dS within the space-time kernel) (Figure 3C). It follows that to create the nearest neighbour in time (NNT) and space-time (NNST) interpolation, we use residuals of the satellite point closest in time and spacetime to the point of interest (lowest dT and dST within the space-time kernel respectively; Figure 3D- 3E). Finally, after interpolation to the animal tracking fix, we then add the satellite residuals with the CHAOS-7 model estimates at ground altitude for the core, lithosphere, and magnetosphere contributions to get the final MagGeo output.

$$MG = SW_s^{Res} + CH_g \quad [3]$$

Thus, to create a complete model of the geomagnetic field for a 3-D location and timestamp of an animal tracking fix which includes core, crustal, ionospheric and magnetospheric contributions, MagGeo combines model estimates and satellite residuals. For simplicity, we will refer to the fused model estimate and satellite residual outputs as MG and the CHAOS-7 model estimates at ground altitude as CH for the remainder of the paper. We can use MG and CH values measured in the North-East-Centre (NEC) coordinate system to calculate the four components of the geomagnetic field that are relevant for animal migration (FHID). We perform our error analysis on these components as their values are more applicable to MagGeo users whose primary objective will likely focus on movement ecology research questions. For a similar geophysical-centered error analysis on the XYZ orthogonal components of geomagnetic model estimates, readers can refer to Beggan (2022).

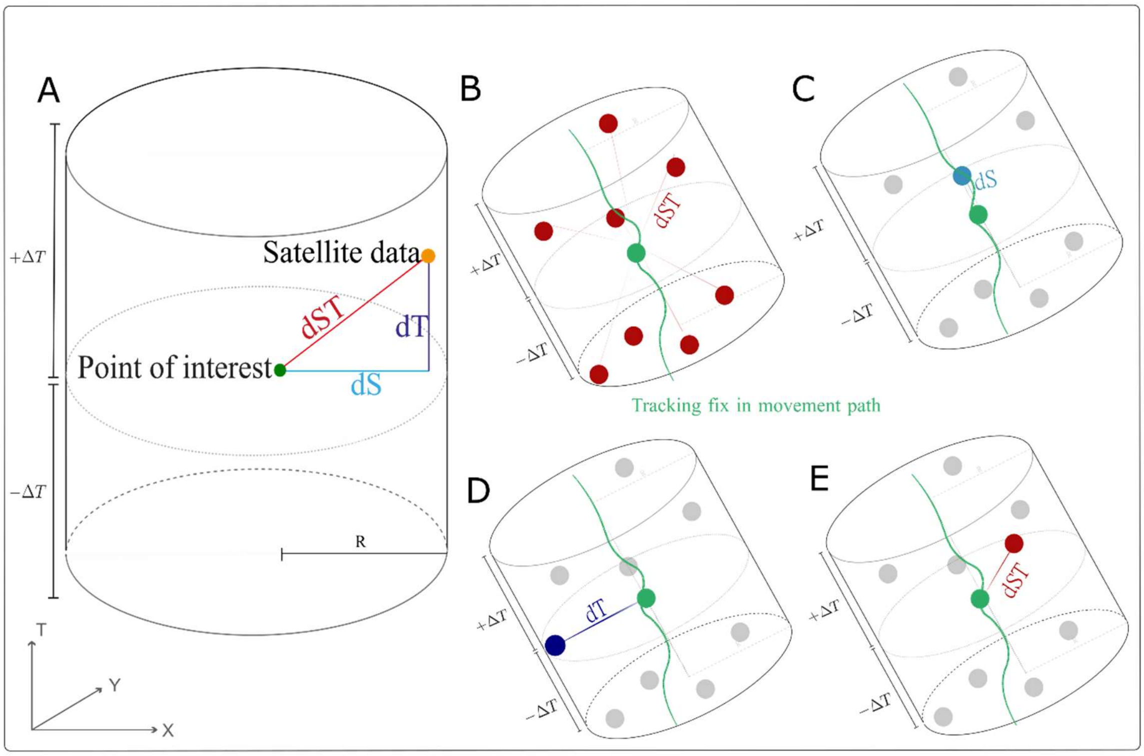

Figure 3. Current and modified spatiotemporal parameters of the spacetime cylinder used by MagGeo. **A.** The space-time cylinder calculating the distance in space (dS; light blue), time (dT; dark blue) and spacetime (dST; red) between point of interest (green) and satellite point (orange). X and Y axis represent spatial dimensions whereas the Z-axis represents temporal dimension. Figures **B-D** represent the four spatiotemporal interpolation methods used to attach satellite geomagnetic data (residuals) to an animal tracking fix (such as movement path of a migratory bird collected by a GPS tag). Figure **B** represents the concept of inverse-distance weighting and Figures **C-E** represent nearest neighbour iterations for satellite points closest to the animal tracking fix in space (**C**), time (**D**) and spacetime (**E**).

2.1 Data Preparation

Our analysis centers on the assumption that data from INTERMAGNET observatories represent the best available measurement of the geomagnetic field at their location on the Earth's surface (Beggan, 2022; Kerridge, 2001). Data from these terrestrial observatories are acutely influenced by the local crustal field, which is not captured by model estimates or satellite data but might be detected by animals moving at this local spatial scale. Additionally, INTERMAGNET observatories collect high temporal resolution geomagnetic data and are rigorously calibrated (Kerridge, 2001). We compare geomagnetic values from INTERMAGNET observatories (OBS) against MG outputs interpolated to the station location for the same timestamp. The objective is to compare MG and OBS values for the four geomagnetic components (F, H, D, I) to assess MagGeo accuracy at ground altitude. Our analysis is conceptually consistent with geophysical studies that test, calibrate and validate satellite (Beggan et al., 2013; Macmillan & Olsen, 2013; Ridley & Macmillan, 2014) and model data (Chulliat et al., 2015; Finlay et al., 2020).

We acquired minute-mean observatory geomagnetic data for all available stations for seven years (2014-2020). We compiled a dataset to test MagGeo under the full range of geomagnetic activity levels (i.e., Kp 0 – 9). We term this dataset "All Kp." We included data from 60 days a year uniformly sampled across all twelve months for seven years resulting in a total of 420 days of data. We obtained geomagnetic data at three time points each day equally spaced 8 hours apart (Table 1). We had fewer INTERMAGNET stations for later years as there is usually a delay between station measurements and access to the final geomagnetic dataset.

To test MagGeo specifically during periods of high geomagnetic activity, we compiled a "High Kp" dataset. To build the High Kp dataset, we acquired data for all days in 2014-2020 with high geomagnetic activity (Kp > 6 for 6 or more hours) (Space Weather Live, 2021). We subset this dataset to include only data where the satellite recorded Kp > 6 to further filter out quieter periods even during a day classified as having overall high geomagnetic activity. The High Kp dataset (n = 393,054) was substantially smaller than the All Kp dataset (n = 6,327,537). There were fewer days with High Kp in 2014 and in 2018 to 2020. These periods were less geomagnetically active as they were in the quieter part of previous solar cycle (Kakad et al., 2020).

Table 1. Datasets used for MagGeo error and accuracy analysis. All data are minute-mean for 2014 to 2020. All Kp includes data from all Kp levels whereas High Kp includes only data from geomagnetically active periods (Kp>6)

Year	All Kp	High Kp	INTERMAGNET stations
2014	899 967	8 602	109
2015	950 346	206 448	111
2016	1 044 477	78 467	103
2017	1 023 750	65 259	100
2018	892 808	26 363	95
2019	888 681	7 915	97
2020	627 508	8 602	88
n total	*6,327,537*	*393,054*	

2.2 Accuracy Assessment

To test the performance of the different spatiotemporal interpolation strategies and data structures relative to one another we used two accuracy measures. The first is the absolute difference (*d*) between the MagGeo output (X_{mg}) and the corresponding observatory value (X_{obs}) for each timestamp:

$$d = |X_{mg} - X_{obs}| \quad [4]$$

Lower values of absolute error correspond to better agreement between the MagGeo output and the INTERMAGNET data.

The second measure (alpha; α) is the absolute difference between the standardized MagGeo output and the standardized observatory output for each timestamp (Ridley & Macmillan, 2014):

$$\alpha = \left|\left(\frac{X_{mg}-\overline{X}_{mg}}{\sigma_{mg}}\right) - \left(\frac{X_{obs}-\overline{X}_{obs}}{\sigma_{obs}}\right)\right| \quad [5]$$

Where $\overline{X}_{mg}$ and σ_{mg} are the mean and standard deviation respectively for the interpolated MagGeo values at a station while $\overline{X}_{obs}$ and σ_{obs} are the mean and standard deviation respectively of the INTERMAGNET values at the same station. As with the absolute difference measure, lower alpha values correspond to better agreement between the MagGeo output and observatory values. The alpha measure is useful for identifying how well MagGeo captures relative patterns in the geomagnetic data instead of just the absolute difference. For example, during a geomagnetic storm, both $X_{mg}$and X_{obs} are very different from their respective means ($\overline{X}_{mg}$ and $\overline{X}_{obs}$). While the absolute difference between $X_{mg}$and X_{obs} might be large during these storms, if the sudden change in geomagnetic value is captured by both sources, the α value will be low thus making it possible for MagGeo outputs and observatory outputs to have high absolute difference error but low alpha values. In this case, the pattern would suggest that MagGeo is able to capture the temporally dynamic nature of the geomagnetic field like the observatory data irrespective of any consistent offsets between the two sources.

We removed data from 8 stations (Figure S1) because their absolute difference error was consistently greater than 2 standard deviations (95% quantile) for any three of the orthogonal components (eg., DIF, XYZ or DHZ) for more than 6 months' worth of data (Beggan, 2022). We also removed data from 3 days (2017-09-08, 2018-08-26, and 2018-08-27) which had high daily error across all stations reflecting the impact of very strong geomagnetic storms on these days.

We calculated the error measures (*d* and *α*) for MagGeo values for each spatiotemporal interpolation method (IDW, NNT, NNS, and NNST) and underlying data structure (CH and MG). We compare across interpolation methods and data structure using summary statistics, but also by recording the proportion of data records where each interpolation method and data structure had the lowest error values ("best performance"). We calculated Pearson's correlation coefficients to compare the best performing MagGeo algorithm with observatory values overall at each station for each geomagnetic component.

We fit generalized linear mixed-effect models (GLMMs) with the dependent variable as either error metric (*d* and *α*) and by using data values from the best performing interpolation method and data structure combination. To reduce temporal autocorrelation, we created hourly averages from our minute-mean data resulting in a total of 107,116 data points. For fixed effects, we included three variables that account for geomagnetic field behaviour: Kp, time of day, and latitude. For simplicity, we categorized time-of-day into two categories: day as 7:00AM to 7:00PM local time and night as 7:00PM to 7:00AM local time to allow sufficient variation in sunset and sunrise times for stations differing by latitude. Solar wind influences the geomagnetic field activity and is reflected as a high Kp value which is more likely during the day and at polar latitudes (Campbell, 2003; Hulot et al., 2010; Lanza & Meloni, 2006). We also included two additional fixed effects in our model that address how MagGeo space-time kernel parameters may influence error: the geographical distance between the INTERMAGNET station and the satellite data point (km) and the temporal difference (minutes) between the timestamp at the INTERMAGNET station data and the nearest Swarm satellite pass.

We used station ID (n=109) as a random effect for all models as it is likely that values from individual ground stations are heavily influenced by local crustal field conditions (Beggan, 2022;

Lesur et al., 2016). Additionally, each station has subtle differences in collection and reporting of geomagnetic data (St-Louis, 2012). We tested all possible combinations of the fixed effects and chose the best model for each geomagnetic component based on the lowest Akaike information criterion (AIC) values. In addition to the coefficient values (β), standard error (SE) and p-values, we also calculated the marginal and conditional R^2 values for the best performing models. Marginal (R^2m) is the proportion of the variance explained by the fixed effects, and the conditional R^2 (R^2c) is the overall proportion of the variance explained by both the fixed and random effects (Nakagawa & Schielzeth, 2013).

To demonstrate the difference between the geomagnetic data sources for studying long-distance animal migration, we used GPS tracking data from one White Stork *Ciconia ciconia* individual from the 2017 spring migration period (Carlson et al., 2021). We resampled the tracking data to hourly intervals when the bird was in flight (speed > 5 km/h) as this state likely reflects when birds are using geomagnetic field values to make movement decisions (Acácio et al., 2022; Chernetsov, 2017). We attached geomagnetic values from the nearest INTERMAGNET station to the bird's location. We compared these observatory values with the MagGeo outputs from the best performing interpolation method and data structure for the same location.

2.3 Tools and data availability

MagGeo is available as a GitHub repository (Benitez & Long, 2022). For our analysis, we modified scripts from MagGeo 1.0 (Feb 2021). MagGeo uses two Python packages for geomagnetic data acquisition. The ESA-VirES Client package connects to the VirES servers to acquire satellite residuals (Smith, 2020) whereas the chaosmagpy package accesses the CHAOS-7 model estimates through the VirES server (Kloss, 2021). We used the Swarm Magnetic Earth Jupyter notebooks to fetch geomagnetic data from ground observatories which we accessed via the

British Geological Survey FTP server, though a VirES-based access method is currently available as well (https://github.com/Swarm-DISC/Swarm_notebooks). To fit our general linear mixed-effect models, we used the "lme4" R package (Bates, 2010). Finally, we used the "dredge" function from the "MuMIn" R package to test all possible combinations of fixed effects (Bartoń, 2022). We accessed White Stork GPS data from Carlson et al. (2021) which are available on Movebank (Kays et al., 2022).

3. Results

For each of the four spatiotemporal interpolation methods, there was little variation in the median, mean, standard deviation, or skew across all geomagnetic components, for both accuracy measures and during variable (All Kp) and high geomagnetic activity (High Kp) (Table 2). The variation in mean absolute difference between the four interpolation methods was within 10 nT for scalar intensity geomagnetic components (F and H) and within 1 degree for angular directional geomagnetic components (D and I) (Table 2). Furthermore, almost all categories showed positive skew (with median <mean), suggesting that mean values may be influenced by a few data points with unusually high error. For both scalar components, while values between the interpolation methods were similar, NNT often had the highest median and mean values. Across each data record (unique location and timestamp) however, the nearest neighbour in time method always had the highest occurrence (%) of lowest error ("best performance") for all components during periods of variable and high geomagnetic activity (Table 3). This distinction was more evident during variable geomagnetic activity where NNT had the lowest error about 40% of the time among the four interpolation methods compared to periods of high geomagnetic activity where NNT on average had the lowest error 30% of the time (Table 3). Thus, all interpolation methods had similar central tendencies (Table 2), but NNT consistently had the best performance (Table 3). Therefore, we used the NNT interpolation method to subsequently test the difference between CH and MG

When separated by station and arranged by latitude, we found that certain stations have greater variation in error than others (large interquartile range for individual station box plot) (Figure 4 and S2). In general, stations at higher latitudes have a greater variation in differences compared to stations closer to the equator. We also observe that these error patterns are consistent between the four interpolation methods such that if a station has high error variability for total intensity, this pattern will be replicated across all interpolation methods (Figure 4 and S2).

Between the two data structures, there was little variation in the median, mean, standard deviation, or skew across all geomagnetic components, for both accuracy measures and during variable (All Kp) and high geomagnetic activity (High Kp) (Table 4). With a few exceptions, difference between CH and MG for the mean and median absolute difference error was approximately within 10 nT for the scalar components and within 1 degree for the angular components (Table 4). For the absolute difference error metric, apart from horizontal intensity, CH had equal or lower median and mean error than MG (Table 4). During both variable and high geomagnetic activity however, MG had either equal or lower mean and median alpha values. Positive skew during variable geomagnetic conditions is also higher for MG alpha values suggesting that the reported mean is being skewed by a few instances of very high error (Table 4).

For 11 out of 16 categories based on geomagnetic components and activity, MG has slightly better performance than CH (Table 5). However, there is little difference in performance across all geomagnetic components, activity and accuracy measures since the overall average performance is 48.3% for CH and consequently 51.7% for MG. The average alpha error per station is also around 1 unit during variable geomagnetic activity and slightly higher during high geomagnetic activity (Figure 5 and Figure S3). Except for declination, MG has lower station-wide alpha error than CH (Figure 5 and Figure S3). Additionally, there is a log-linear increase in Swarm satellite contribution to the MG data (e.g., increasing residual values) associated with an increase in geomagnetic activity (Figure S4).

When using the best performing MagGeo algorithm (NNT interpolation and MG data structure), MagGeo values for all geomagnetic components were overall highly correlated with observatory values overall (r >0.9 for FHID). Out of 109 stations and for all geomagnetic components, at least 50% of all stations had correlation values greater than 0.5 though the percentage of stations varied by geomagnetic component (F: 88%, H: 53%, D: 78% and I: 66% of stations had correlation values greater than 0.5) (Figure S5). Horizontal intensity and inclination had the lowest number of stations with high correlations though stations with low correlations were typically at higher latitudes.

Table 2. Median, mean, standard deviation and skew of error for current and modified MagGeo spatiotemporal interpolation methods: IDW, NNS, NNST and NNT. Results are for all geomagnetic components (FHID) with minute-mean data from 2014-2020. "All Kp" includes data from all Kp levels whereas "High Kp" includes only data from geomagnetically active periods (Kp>6). Results are presented for both accuracy measures: absolute difference (*d*) and alpha (*α*).

	d								***α***							
	All Kp				**High Kp**				**All Kp**				**High Kp**			
Component	*Median*	*Mean*	*± SD*	*Skew*	*Median*	*Mean*	*± SD*	*Skew*	*Median*	*Mean*	*± SD*	*Skew*	*Median*	*Mean*	*± SD*	*Skew*
Total intensity																
IDW	79.2	127.4	135.4	2.1	101.5	258.8	592.3	6.0	0.5	0.7	0.8	2.4	0.8	1.0	0.8	2.6
NNS	79.4	127.4	135.0	2.1	101.6	259.7	593.2	5.9	0.5	0.7	0.8	2.3	0.8	1.0	0.9	5.2
NNST	79.4	127.6	135.3	2.1	100.8	258.6	592.5	5.9	0.5	0.7	0.8	2.4	0.8	1.0	0.9	4.2
NNT	79.7	128.0	135.7	2.1	108.4	267.3	591.3	5.9	0.5	0.8	0.8	2.7	0.8	1.0	0.9	4.0
Horizontal intensity																
IDW	211.3	211.2	133.1	1.0	284.4	371.1	393.2	4.1	0.6	0.9	0.9	2.8	0.9	1.1	0.9	2.0
NNS	211.5	211.7	134.0	1.1	284.3	374.1	401.3	4.0	0.6	0.9	0.9	2.9	0.8	1.0	0.9	4.5
NNST	211.7	212.0	134.2	1.1	285.5	375.6	401.7	4.0	0.6	0.9	0.9	2.9	0.9	1.0	0.9	3.6
NNT	211.5	211.9	133.4	1.0	298.0	382.8	392.6	4.0	0.6	0.9	0.9	2.9	0.9	1.1	0.9	3.6
Inclination																
IDW	0.3	0.3	0.2	2.6	0.4	0.5	0.5	4.0	0.6	0.8	0.9	2.9	0.9	1.1	0.9	2.0
NNS	0.3	0.3	0.2	2.6	0.4	0.5	0.5	4.0	0.6	0.8	0.9	3.0	0.8	1.0	0.9	4.7
NNST	0.3	0.3	0.2	2.6	0.4	0.5	0.5	4.0	0.6	0.8	0.9	3.0	0.8	1.0	0.9	3.6
NNT	0.3	0.3	0.2	2.6	0.4	0.5	0.5	4.0	0.6	0.8	0.9	2.9	0.9	1.1	0.9	3.6
Declination																
IDW	0.1	0.4	0.6	3.8	0.3	0.9	2.4	13.2	0.7	0.9	0.8	2.2	0.9	1.0	0.9	2.3
NNS	0.2	0.4	0.7	3.6	0.3	0.9	2.4	12.1	0.7	0.9	0.9	2.3	0.8	1.0	0.9	5.4
NNST	0.2	0.4	0.7	3.6	0.3	0.9	2.4	12.2	0.6	0.9	0.8	2.4	0.8	1.0	0.9	4.1
NNT	0.2	0.4	0.7	3.7	0.3	1.0	2.5	10.9	0.7	0.9	0.9	2.7	0.8	1.0	0.9	4.2

Table 3. Percent of lowest error between four MagGeo spatiotemporal interpolation methods: IDW, NNS, NSST, and NNT. Bolded rows represent the interpolation method that had the overall highest frequency of lowest error (best performance). Results shown for all geomagnetic components (FHID) with minute-mean data from 2014-2020. "All Kp" includes data from all Kp levels whereas "High Kp" includes only data from geomagnetically active periods (Kp>6). Results are for both accuracy measures: absolute difference (*d*) and alpha (*α*).

	Percent (%) with lowest error			
	All Kp		**High Kp**	
Component	*d*	*α*	*d*	*α*
Total Intensity				
IDW	17.8	18.5	22.0	**27.8**
NNS	31.4	19.3	33.4	22.7
NNST	8.4	22.5	5.6	22.4
NNT	**42.4**	**39.7**	**39.1**	27.2
Horizontal intensity				
IDW	19.4	18.6	21.5	22.6
NNS	30.8	20.4	34.2	24.8
NNST	8.9	19.9	5.3	22.4
NNT	**40.9**	**41**	**39.1**	**30.2**
Inclination				
IDW	19	19.5	20.9	23.2
NNS	30.6	19.9	34.1	24.5
NNST	8.7	21.1	5.0	22.9
NNT	**41.7**	**39.4**	**39.9**	**29.5**
Declination				
IDW	21.3	20.3	26.8	25.8
NNS	30.5	19.5	32.9	24.6
NNST	8.2	20.7	5.1	21.7
NNT	**40.1**	**39.5**	**35.2**	**27.9**

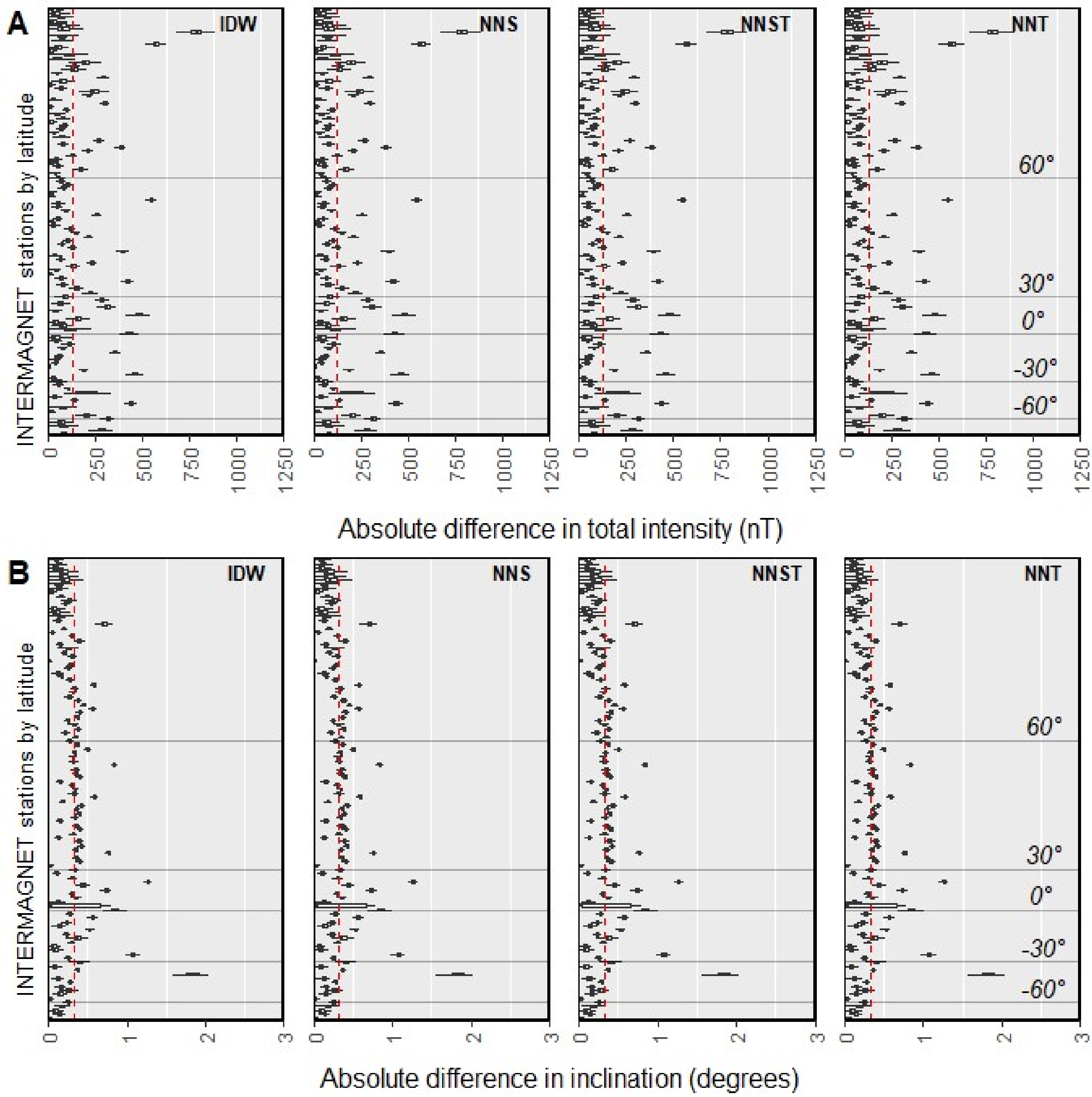

Figure 4. Absolute difference metric (*d*) for each individual INTERMAGNET station arranged by latitude from northernmost (top) to southernmost (bottom). Each panel represents one of the four possible MagGeo spatiotemporal interpolation methods: IDW, NNS, NNST and NNT. Dotted red lines represent overall average absolute difference. Figures are arranged by geomagnetic component: total intensity (**A**) and inclination (**B**). For similar figures for horizontal intensity and declination, see Figure S2.

Table 4. Median, mean, standard deviation and skew of error for current and modified MagGeo data structures: CH (CHAOS-7 estimates) and MG (CHAOS-7 estimates and Swarm residuals). Results are for all geomagnetic components (FHID) with minute-mean data from 2014-2020. “All Kp” includes data from all Kp levels whereas “High Kp” includes only data from geomagnetically active periods (Kp>6). Results are for both accuracy measures: absolute difference (*d*) and alpha (*α*).

	d								***α***							
	All Kp				**High Kp**				**All Kp**				**High Kp**			
Component	*Median*	*Mean*	*± SD*	*Skew*	*Median*	*Mean*	*± SD*	*Skew*	*Median*	*Mean*	*± SD*	*Skew*	*Median*	*Mean*	*± SD*	*Skew*
Total intensity																
CH	78.6	126.9	135.3	2.1	105.0	261.8	595.3	5.9	0.6	0.8	0.8	2.1	1.0	1.1	0.8	0.9
MG	79.7	128.2	153.8	65.8	108.4	267.3	591.3	5.9	0.5	0.8	0.2	3.7	1.0	1.1	0.8	1.0
Horizontal intensity																
CH	212.0	211.1	131.7	1.0	297.8	365.9	379.6	4.5	0.8	1.0	0.8	2.1	1.0	1.1	0.9	1.0
MG	211.7	212.4	134.9	2.1	298.0	382.8	392.6	4.0	0.6	0.9	1.0	3.7	0.9	1.1	0.9	1.3
Inclination																
CH	0.3	0.3	0.2	2.6	0.4	0.5	0.5	4.1	0.7	0.9	0.8	2.2	1.0	1.1	0.8	1.0
MG	0.3	0.3	0.2	3.7	0.4	0.5	0.5	4.0	0.6	0.8	0.9	3.7	0.9	1.1	0.9	1.2
Declination																
CH	0.1	0.3	0.6	3.9	0.2	0.8	2.3	13.8	0.7	0.9	0.8	1.8	1.0	1.1	0.8	1.0
MG	0.2	0.4	0.7	4.1	0.3	1.0	2.5	10.9	0.7	0.9	0.9	3.3	0.9	1.1	0.9	1.2

Table 5. Percent of lowest error between two MagGeo data structures: CH (CHAOS-7 estimates) and MG (CHAOS-7 estimates and Swarm residuals). Bolded rows represent the data type that had the highest percentage of lowest error for each category (best performance). Results are for all geomagnetic components (FHID) with minute-mean data from 2014-2020. "All Kp" includes data from all Kp levels whereas "High Kp" includes only data from geomagnetically active periods (Kp>6). Results are for both accuracy measures: absolute difference (*d*) and alpha (*α*).

Component	**Percent (%) with lowest error**			
	All Kp		**High Kp**	
	d	*α*	*d*	*α*
Total Intensity				
CH	**52.8**	41	**50.8**	48.9
MG	47.2	**59**	49.2	**51.1**
Horizontal intensity				
CH	47.9	40.8	47.6	48.6
MG	**52.1**	**59.2**	**52.4**	**51.4**
Inclination				
CH	**50.7**	41.4	47.3	48.1
MG	49.3	**58.6**	**52.7**	**51.9**
Declination				
CH	**55.6**	48	**58.2**	45.3
MG	44.4	**52**	41.8	**54.7**

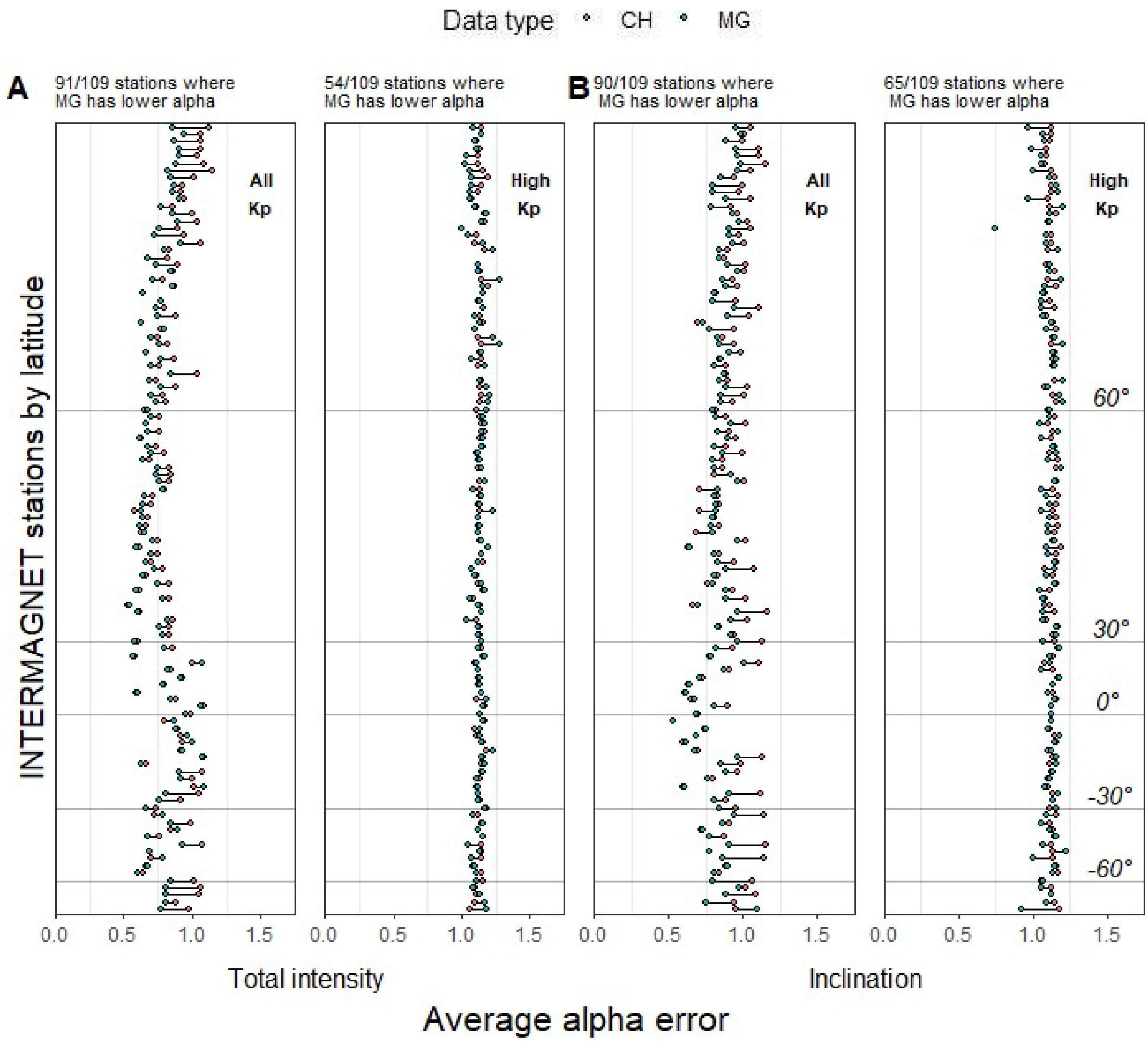

Figure 5. Comparison of average alpha measure (α) between CH (red dots) and MG (blue dots) for each individual INTERMAGNET station arranged by latitude from northernmost (top) to southernmost (bottom). “All Kp” includes data from all Kp levels whereas “High Kp” includes only data from geomagnetically active periods (Kp>6). Individual plot titles indicate count of stations where MG had lower alpha error. Figures are arranged by geomagnetic component: total intensity (**A**) and inclination (**B**). For similar figures for horizontal component of intensity and declination, see Figure S3.

3.1 Factors influencing error and accuracy structure

For distance in space, most satellite data points are between 1000-1250 km away from the INTERMAGNET station (Figure 6). This pattern might be a result of the clustering of stations at mid-latitudes in Europe (Figure 2 and 6B) who will have similar space-time kernel parameters and subsequently error. The low hourly error at smaller distances might reflect that MagGeo can accurately capture geomagnetic patterns if the satellites are close in space to the INTERMAGNET station (Figure 6A). Conversely, the low hourly error at high distances might be indicative of stations near the equator who have larger space-time kernels but are also found at latitudes where there is lower geomagnetic activity (Figure 6B).

There is little overall variation in the distance in time between the INTERMAGNET station and satellite data point though there are two peaks at 0-30 minutes and 190-220 minutes (Figure 7). This clustering is likely related to the +/- 4-hour parameter of the space-time kernel where the nearest satellite data point is either directly above the INTERMAGNET station (0-30 minutes) or will just meet the +/-4-hour cut-off by either passing over the INTERMAGNET station 4 hours ago or passing over it 4 hours later (190-220 minutes).

Random effects (individual stations) and fixed effects (geomagnetic activity and time of day) together explain most of the absolute difference between geomagnetic values collected at INTERMAGNET stations and outputs from MagGeo (conditional R^2 is close to 0.9-1.0 for all geomagnetic components, Table 6). Apart from inclination (marginal R^2 is 0.5), variation at individual stations (random effects) explains most of the difference (marginal R^2 is equal to or below 0.1). Generally, INTERMAGNET data from stations at higher absolute latitudes are consistently different from MagGeo outputs, especially for the angular directional geomagnetic components such as inclination and declination (Table 6, Figure 4B).

Random and fixed effects do not explain most of the variation in the alpha error (conditional R^2 is equal to 0.11, Table 7). For these models however, fixed effects explain all the difference between MagGeo outputs and INTERMAGNET stations (marginal R^2 equal to conditional R^2, Table 7). For example, for all geomagnetic components, high geomagnetic activity leads to higher error (Table 7). These models also suggest that alpha error is higher during the day compared to nighttime. None of the best models (lowest AIC) for any geomagnetic component with absolute difference as a dependent variable have distance in space as a fixed effect (blank rows in Table 6) whereas only total intensity and inclination have distance in time included as a fixed effect. This is in contrast with the best models with alpha error as a dependent variable since almost all components have both distance in space and time as fixed effects in their models. While not always statistically significant, in models where these variables are included distance in space and time between satellite pass and INTERMAGNET station have an impact on error such that an increase in distance leads to larger alpha error.

Table 6. Results of the generalized linear mixed-effect models of absolute difference as dependent variable, individual station as a random effect and fixed effects as Kp, absolute value of latitude, time of day and distance in space and time between satellite and point of interest. R^2m and R^2c refer to marginal and conditional R^2 respectively. A new model was fit for each geomagnetic component (FHID). Models are fit with combined model estimate and satellite residual data and NNT interpolation during periods of variable geomagnetic activity (All Kp). Minute-mean data are averaged into hourly values, and empty rows indicate that the fixed effect did not contribute to the final model (based on lowest AIC) for that geomagnetic component.

	Total intensity			**Horizontal intensity**			**Inclination**			**Declination**		
	β	**SE**	**p**	**β**	**SE**	**p**	**β**	**SE**	**p**	**β**	**SE**	**p**
Intercept	71.3	36.3	0.05	245.6	32.6	<0.01	-33.0	1.3	<0.01	-0.2	0.1	0.2
Kp	1.6	0.1	<0.01	5.5	0.1	<0.01	0.007	1.3E-04	<0.01	0.02	5.9E-04	<0.01
Absolute Latitude	1.4	0.8	0.07	-1.1	0.7	0.1	0.7	0.01	<0.01	0.01	0.003	<0.01
Time of day (Ref: Day)												
Night	0.8	0.2	<0.01	4.7	0.3	<0.01	0.008	3.3E-04	<0.01	-0.004	0.001	0.01
Distance (km)												
Time difference (min)	-0.003	0.0	0.03				-3.8E-06	2.4E-06	0.1			
R^2m	0.03			0.02			0.5			0.1		
R^2c	1.0			0.9			1.0			0.9		

Table 7. Results of the generalized linear mixed-effect models of alpha measure as dependent variable, individual station as a random effect and fixed effects as Kp, absolute value of latitude, time of day and distance in space and time between satellite and point of interest. R^2m and R^2c refer to marginal and conditional R^2 respectively. A new model was fit for each geomagnetic component (FHID). Models are fit with combined model estimate and satellite residual data and NNT interpolation during periods of variable geomagnetic activity (All Kp). Minute-mean data are averaged into hourly values, and empty rows indicate that the fixed effect did not contribute to the final model (based on lowest AIC) for that geomagnetic component.

	Total intensity			**Horizontal intensity**			**Inclination**			**Declination**		
	β	**SE**	**p**	**β**	**SE**	**p**	**β**	**SE**	**p**	**β**	**SE**	**p**
Intercept	0.5	0.1	<0.01	0.5	0.03	<0.01	0.3	0.06	<0.01	0.8	0.01	<0.01
Kp	0.2	0.002	<0.01	0.2	0.002	<0.01	0.2	0.002	<0.01	0.1	0.002	<0.01
Absolute Latitude	-9.1E-04	6.4E-04	0.2				0.003	5.5E-04	<0.01			
Time of day (Ref: Day)												
Night	-0.1	0.005	<0.01	-0.2	0.005	<0.01	-0.1	0.005	<0.01	-0.3	0.01	<0.01
Distance (km)	4.4E-05	2.8E-05	0.1	4.2E-05	2.5E-05	0.1	4.4E-05	3.0E-05	0.1			
Time difference (min)	3.3E-04	3.4E-05	<0.01	1.8E-04	3.8E-05	<0.01	2.0E-04	3.6E-05	<0.01	2.5E-04	3.7E-05	<0.01
R^2m		0.1			0.1			0.1			0.1	
R^2c		0.1			0.1			0.1			0.1	

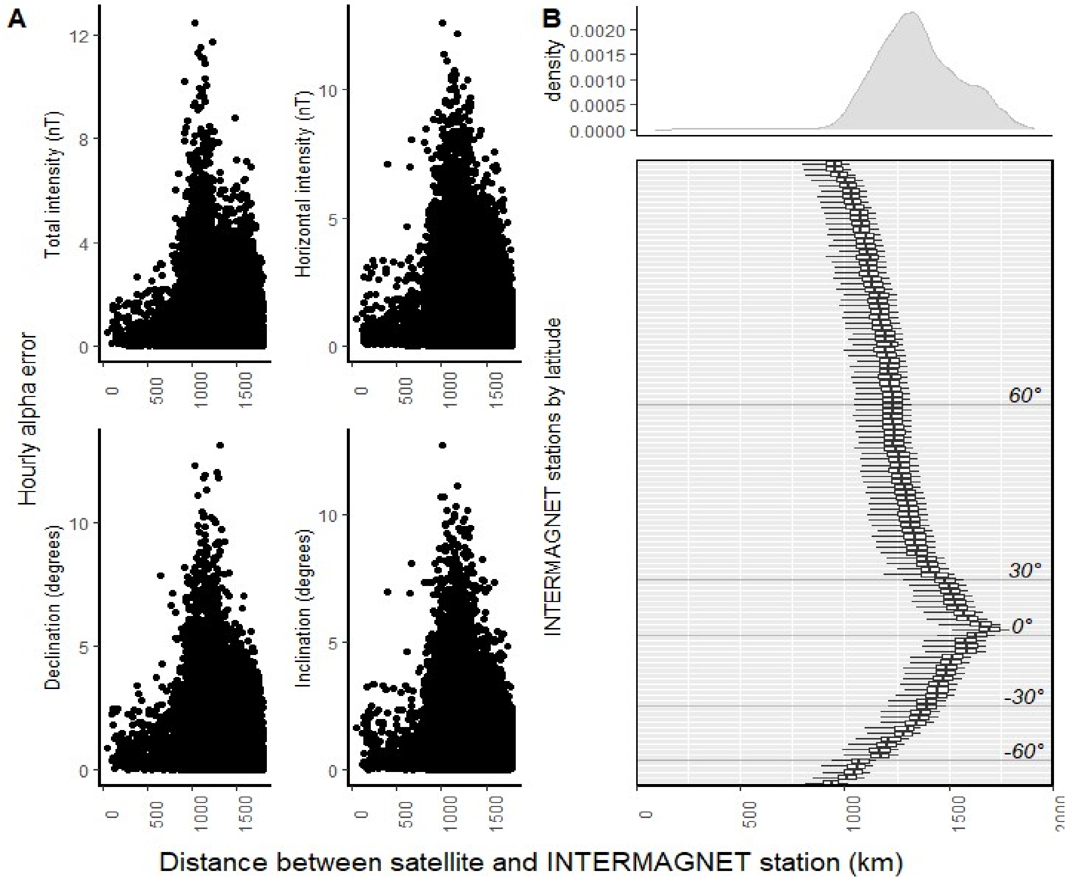

Figure 6. Distance in space between satellite pass and INTERMAGNET station (km) where **(A)** shows the distribution of hourly alpha error for each geomagnetic component (FHDI) and **(B)** shows the spread of the distance values for each individual station arranged by latitude from northernmost (top) to southernmost (bottom). Density plot in **(B)** mirrors the pattern seen in **(A)** where most distance values are between 1000-1500 km. Data are combined model estimate and satellite residual and interpolated to the station location using a NNT method during periods of variable geomagnetic activity (All Kp).

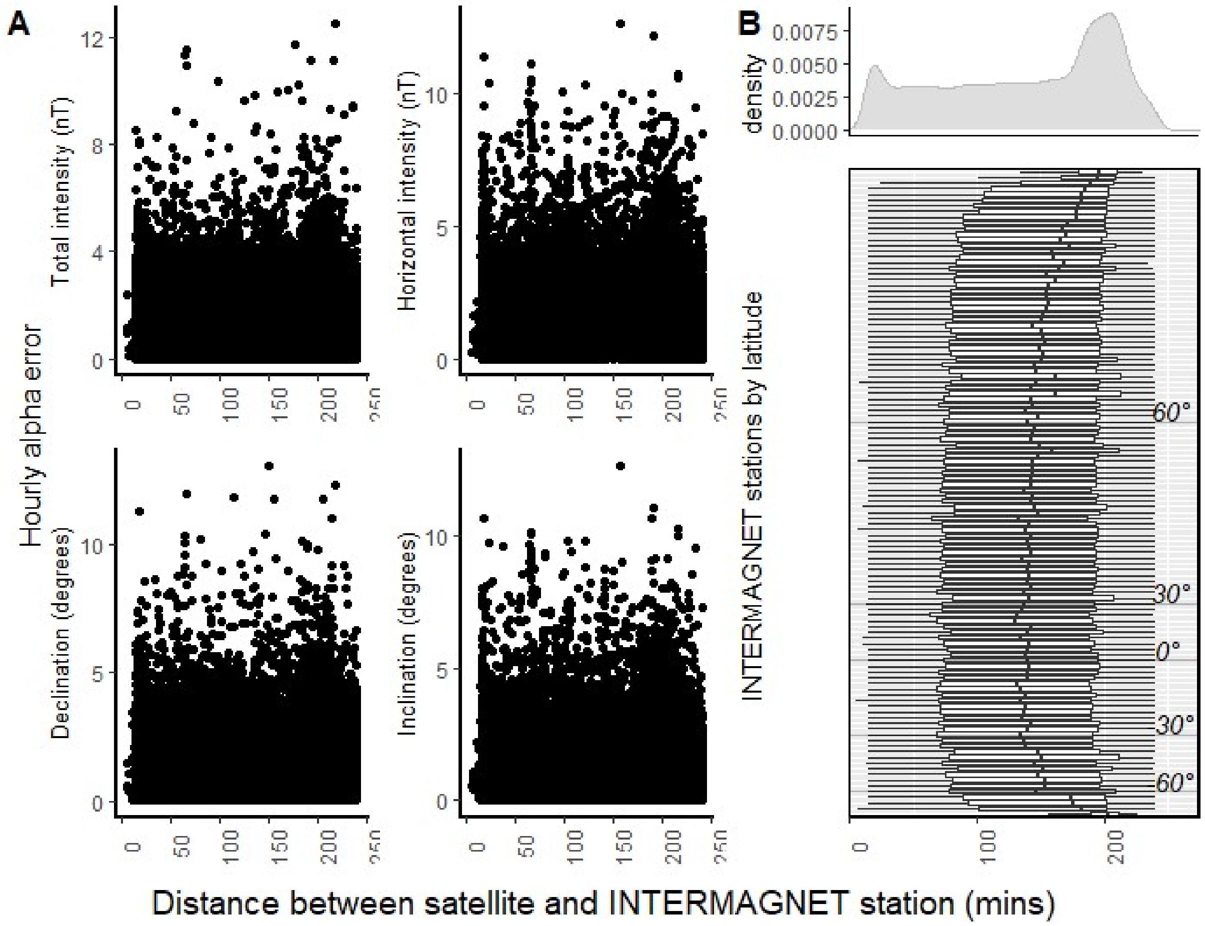

Figure 7. Time difference (mins) between satellite pass and INTERMAGNET station timestamp where **(A)** shows the distribution of hourly alpha error for each geomagnetic component (FHDI) and **(B)** shows the spread of time difference for each individual station arranged by latitude from northernmost (top) to southernmost (bottom). Data are combined model estimate and satellite residual and interpolated to the station location using a NNT method during periods of variable geomagnetic activity (All Kp).

3.2 Attaching geomagnetic data to a migratory bird track

We used movement data collected by a GPS tag carried by one White Stork individual during spring migration as it moves from its wintering grounds in sub-Saharan Africa to its breeding grounds in northeastern Europe by crossing the Sahara Desert. Due to the limited number of stations in Africa, the distance between the bird's location and the nearest INTERMAGNET station is high. This distance decreases as the bird nears its breeding grounds in Europe where there is high station density. In this region, attaching data from the nearest INTERMAGNET station to the bird's location effectively mirrors a continuous geomagnetic data surface. For example, in the later stages of the bird's migration (after Julian Day 90), the curved lines at the northern latitudes using observatory values appears like the curved lines using MagGeo outputs. MagGeo outputs however use continuous model estimates across the world and can represent the changes in geomagnetic values at every location as the bird moves across large distances. Even when including the interpolated satellite residuals required to create the MG data framework, the farthest distance between a satellite pass and a bird's location is still lower than the farthest distance between an INTERMAGNET station and a bird's location.

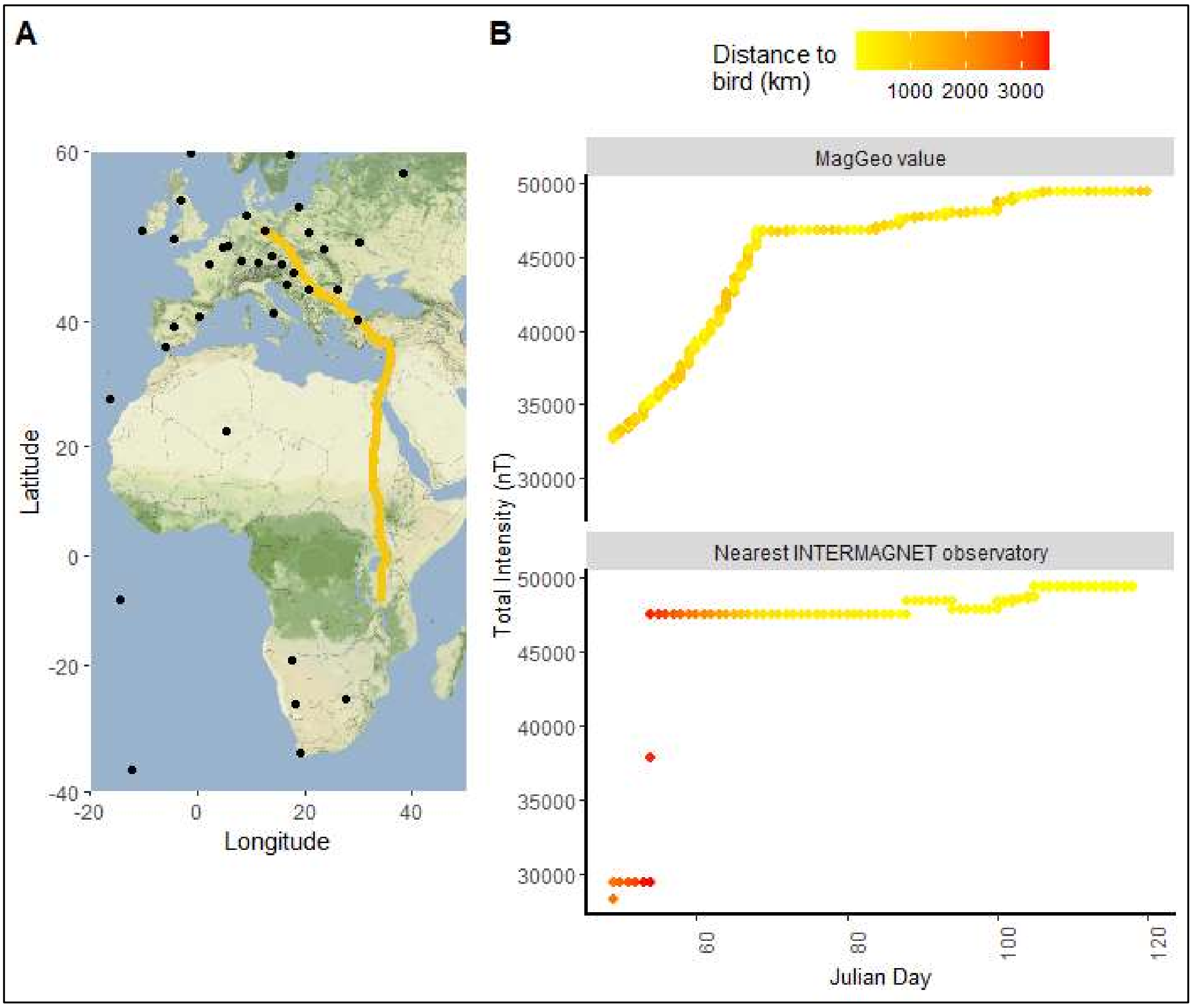

Figure 1. Comparison of geomagnetic data sources for attaching total intensity (nT) values to a movement track of a migratory White Stork individual travelling between its wintering ground in sub-Saharan Africa and its breeding ground in northeastern Europe in spring. **A.** The migratory track (yellow) of a White Stork individual carrying a GPS tag. INTERMAGNET stations are identified with black dots. **B.** Difference between using geomagnetic data from nearest INTERMAGNET station compared to the MagGeo tool output is more evident in locations where there is a lower density of stations (areas outside of Europe). The fused model estimates and satellite residual data framework alongside the nearest neighbour interpolation method of MagGeo ensures a high likelihood of representing the gradient of values experienced by the bird as it moves across long distances.

4. Discussion

The overall absolute difference error was less than 1% of the possible range of values for all geomagnetic components. For example, globally, the total intensity ranges from 23,000 nT to 60,000 nT and the mean and median error were 128nT and 80nT respectively when using the fused model estimate and satellite residual data (MG) framework and NNT interpolation method. While animal sensitivity to geomagnetic values is unclear, these error ranges are well within the possible fluctuations of geomagnetic values during geomagnetic storms (>1000 nT for total intensity) and would also be useful at the assumed sensitivity levels for long-distance migratory animals (Beason & Semm, 1987; Chernetsov et al., 2017; Schwarze et al., 2016; Semm & Beason, 1990). Absolute difference stayed below 1% for all geomagnetic components despite changes to the underlying spatiotemporal interpolation method or geomagnetic data structure. NNT did consistently capture the values and patterns observed at ground observatories better than all other interpolation methods thus having the best overall performance. Generally, MG also captured the patterns observed at stations better than just model estimates (CH) especially during high activity levels. More than 50% of all stations have moderate to high correlation between MagGeo outputs and observatory values in addition to overall correlation being very high across all geomagnetic components. In general, MagGeo accuracy is lower at higher latitudes and during geomagnetically active periods where there is greater influence of solar activity.

In comparison to the Benitez-Paez et al. (2021) who test MagGeo at three INTERMAGNET stations for 6 days in a single year, we test 109 geomagnetic observatory locations across 7 years. Our results suggest that changing MagGeo's underlying spatiotemporal interpolation method from IDW to NNT while continuing to use fused model estimates and satellite residual data will be an improvement to using only model estimates to represent values experienced by animals near the Earth's surface; thus, proving useful for movement ecology studies that test unique research questions regarding the navigational abilities of migratory animals anywhere in the world.

4.1 Interpolation methods

A persistent challenge for the field of remote sensing and movement ecology is how to annotate dynamic environmental covariate data to a moving object (such as a migratory animal) to best model the landscape in a way that accurately represents the animal's experience (Brum-Bastos et al., 2021). This question is addressed by platforms like Movebank (Kays et al., 2022; Kranstauber et al., 2011) and Env-DATA (Dodge et al., 2013) that annotate a movement track with dynamically changing covariates like wind. Env-DATA offers the user with some flexibility for how to interpolate covariate data to the location and timestamp of interest. While the Env-DATA database currently stores information for many different environmental covariates useful for movement ecologists, it does not provide an avenue for attaching geomagnetic data to a movement track.

When Benitez-Paez et al., (2021) developed MagGeo to address this technological gap, they implemented an IDW method to interpolate residuals from satellite data to an animal tracking fix. The assumption was that an average geomagnetic value will reduce the influence of any outlier value on the final geomagnetic outputs (Benitez-Paez et al., 2021). However, compared to any nearest neighbour algorithm, averaging the geomagnetic values through IDW may smooth over the very fluctuations MagGeo hopes to capture. We tested this assumption by testing three simpler nearest neighbour interpolation techniques within the MagGeo framework. We found that the NNT had the best performance since it had the highest percent occurrence of lowest error when compared to values and patterns observed at terrestrial geomagnetic stations part of the

INTERMAGNET network. Attaching residuals from satellite data closest in time to the point of interest like an animal tracking fix will increase the likelihood of capturing the temporal dynamics of the geomagnetic field. The NNT method is also computationally simpler than IDW algorithm. Based on these results and rationale, there is a strong argument for changing MagGeo's underlying spatiotemporal interpolation from IDW to NNT.

It is important to highlight that while we tested different interpolation methods, we maintained the time and space parameters of the existing MagGeo kernel. Benitez-Paez et al. (2021) selected these parameters based on the structure of the polar-orbiting Swarm satellites that pass near a location every four hours with higher clustering of data points at polar latitudes compared to equatorial latitudes due to the radius of the Earth (Friis-Christensen et al., 2006; Olsen et al., 2010). It is important to maintain some function that ensures that temporally contemporaneous geomagnetic data are within a certain spatial distance of an animal tracking fix. Future research may look at what this optimal distance may be to maximize performance, but it is likely that it will vary by latitude like the current implementation.

4.2 Data structure

We found that a combination of CHAOS-7 model estimates and Swarm satellite residuals (MG) can capture relative geomagnetic patterns (lower alpha) observed on the Earth's surface better than using only CHAOS-7 (CH) model estimates. Interestingly, while the satellite data contribution increased as geomagnetic activity increased, this additional residual contribution did not significantly improve the accuracy when comparing with INTERMAGNET stations values (average performance around 50%). This result is surprising since Benitez-Paez et al. (2021) proposed the MG data structure with the expectation that the addition of satellite residuals would capture the temporal variability of the geomagnetic field during periods of higher geomagnetic activity.

Model estimates, which are built primarily from quiet-time data, do not represent geomagnetic values during periods of higher activity such as daytime fluctuations outside of quiet-time or discrete events like geomagnetic storms (Finlay et al., 2020; Thébault et al., 2010). Interpolation of residuals from satellites is then likely to add some of the temporal variability not captured by models (Benitez-Paez et al., 2021). Our results indicate however that overall mean MagGeo error increases during periods of higher geomagnetic activity though a positive skew index suggests that mean error may be influenced by a few exceptionally high error data points. Indeed, a double exponential (Laplacian) distribution with a sharp peak around zero and long tail is expected when comparing geomagnetic model data with ground-based measurements (Walker & Jackson, 2000). For example, when comparing IGRF-13 values against ground-based measurements, Beggan (2022) reported absolute difference error values closely mirroring our results alongside the expected Laplacian distribution.

Additionally, high geomagnetic activity may impact satellite data collection which will consequently impact the satellite residuals used for the MG structure (Babayev et al., 2006; Lanza & Meloni, 2006). For example, we had to remove data from days during known solar storms as the error was particularly high. Additionally, though we used the NNT interpolation method, the residuals from satellite data may reflect values almost 4 hours before or after the geomagnetic storm due to the MagGeo's space-time cylinder parameters (Benitez-Paez et al., 2021). As a result, while the INTERMAGNET station may have recorded geomagnetic values during the geomagnetic storm, MagGeo outputs may not have captured the localised storm especially at high northern latitudes at such a fine temporal resolution given a possible lagged satellite residual.

When combining satellite data and model estimates, we corrected for the difference between satellites collecting geomagnetic data at orbit altitudes and animals experiencing the geomagnetic field at ground altitudes by using model estimates for ground altitudes. The satellite residuals we used however still represent values at orbit altitude and neither our current MagGeo data framework nor interpolation method cannot address this limitation. It is possible to access other geomagnetic model data which, unlike the CHAOS-7 model, provides estimates for all sources of the geomagnetic field. These models do not require correction for the altitude difference (Chulliat et al., 2020; Sabaka et al., 2018, 2020). These values however will not accurately represent the instantaneous and local variability of the geomagnetic field as may be experienced by migratory animals. Incorporating satellite data at satellite altitude will capture some of this variability, and such local variations, especially during geomagnetic storms, are likely to impact orientation by animals using the geomagnetic field (Alerstam, 1987; Benitez-Paez et al., 2021; Schiffner et al., 2011; Wynn et al., 2022; Zein et al., 2022). Further work will be necessary to compare error and accuracy of different models with the MagGeo framework.

During most time periods, our results suggest that MG data can consistently capture geomagnetic patterns well. Indeed, while geomagnetic storm events are uncommon, our results suggest that MG still captures geomagnetic patterns slightly better than CH. Additionally, our accuracy analysis uses data from INTERMAGNET stations collected by well calibrated instruments that have high accuracy and precision especially compared to animals who may sense the geomagnetic field for navigation and orientation purposes (Kerridge, 2001; Mouritsen, 2014; Zein et al., 2021). Furthermore, one of the leading hypotheses for animals using the geomagnetic field is the “gradient hypothesis” where relative patterns in geomagnetic intensity or inclination might be more useful for migratory animals than absolute values (Boström et al., 2012; Kishkinev et al., 2015; Wiltschko & Wiltschko, 2021). Additionally, when using the MG data structure and NNT interpolation method, station-wide correlation is moderate to high for most stations. The overall global correlation between MagGeo outputs and observatory values however, is very high suggesting that MagGeo could be used to study long-distance animal migration which happens on a global scale. Based on these considerations, the algorithm from MagGeo that we implement provides a highly useful and robust framework for attaching geomagnetic data to animal tracking data (Zein et al., 2022).

4.3 Outliers

We found outliers to be particularly informative as they highlighted spatial nuances of the geomagnetic field. Most outliers in our dataset represent locations with unique geomagnetic signatures due to local geophysical properties not captured by model estimates at such an acute scale (e.g. Beggan, 2022). Many of the stations highlighted in Figure S1 are volcanic islands with basaltic composition including high concentrations of ferromagnetic minerals (Johnston, 1989; Thébault et al., 2010). Others like the Bangui magnetic anomaly relate to deep geological structures (Girdler et al., 1992). Such lithospheric anomalies have a large local influence on geomagnetic values which may subsequently impact an animal moving through this geomagnetic landscape. For example, birds passing over the geomagnetic anomaly in Sweden have been previously noted to change their behavior suggesting that animal movement may in fact be influenced by local anomalies (Alerstam, 1987). Similar analyses can be conducted by using open-source resources like the World Digital Magnetic Anomaly Map (WDMAM) which allows users to easily extract anomaly information from a raster layer (Lesur et al., 2016).

As expected, stations located at high northern latitudes consistently exhibit outliers. In general, all geomagnetic components have a larger range of error at the polar latitudes since charged particles ejected from the sun more readily enter the Earth's atmosphere in the auroral zones at the poles (Campbell, 2003). Model estimates, created from quiet-time data, do not capture these changes for any geomagnetic component. However, for long-distance migrants especially near polar latitudes, geomagnetic strategies may not be useful for navigation or orientation as values can be unreliable in both magnitude and sign. The lack of predictability would thus provide little useful information, especially for migratory animals who have high site fidelity (Lohmann et al., 2008; Wynn et al., 2020). Nevertheless, MagGeo's high global accuracy can still be a valuable tool to reliably attach geomagnetic data to animal tracks for studies wishing to test hypotheses specific to this geographic region.

4.4 Limitations

Geomagnetic sensitivity and perception ranges are unknown for most species and to our knowledge, there are no instruments that accurately record geomagnetic conditions as experienced by migratory animals, though there are species-specific estimates (Åkesson et al., 2005; Beason & Semm, 1987; Chernetsov et al., 2017; Schwarze et al., 2016; Semm & Beason, 1990). The most suitable candidate for attaching geomagnetic data to animal movement data would be INTERMAGNET stations which collect high-temporal resolution geomagnetic values at ground altitudes. These stations however do not have a high global density and thus cannot be used to accurately capture the range of geomagnetic values experienced by an animal during long-distance migration. Using GPS tracking data of a White Stork individual, we demonstrate how attaching geomagnetic data from the nearest station to a migratory bird's location might be ideal for locations in Europe. Outside of Europe however, there would likely be a large mismatch between the geomagnetic values experienced by a bird and a station collecting geomagnetic data more than 2,000 km away. Instead, using a combination of model estimates and interpolated satellite residuals could serve as a sufficient alternative that captures high spatiotemporal resolution geomagnetic data for all locations on Earth.

We do use INTERMAGNET station data as the ideal standard to perform our error and accuracy analysis to test our MagGeo tool. We did not however anticipate the level of uncertainty introduced by the station data themselves though this is primarily explained by local crustal fields (Beggan, 2022). Our analyses suggest that MagGeo outputs and observatory values are offset by a unique amount specific to each INTERMAGNET station and our linear mixed-effect models reveal that the majority of the error structure for absolute difference can be explained by these random, location-specific effects (St-Louis, 2012). In addition to geomagnetic activity as a fixed effect, these models explain most of the variation in the error structure for differences between MagGeo outputs and observatory values. These results highlight the limitation of our structural set-up as this station-specific offset skews the absolute difference by a consistent amount for each data record. The alpha measure partly addresses this issue by subtracting the standardized MagGeo outputs from the standardized observatory values (Ridley & Macmillan, 2014). Our linear mixed-effect models fit with alpha as the dependent variable suggest that random, location-specific effects explained much less of the error structure. It is noteworthy however that Kp and time of day influenced the error structure in predictable ways such that periods of high geomagnetic activity lead to higher error (Campbell, 2003; Lanza & Meloni, 2006).

4.5 Applications and open questions

Most of our analysis is from data collected in the last 7 years (2014-2020) which is largely during the quiet period of the current solar cycle (Kakad et al., 2020; Li et al., 2011). The 11-year and 22-year solar cycle has a significant influence on geomagnetic field activity since years of high solar activity correspond to higher occurrence of geomagnetic storms (Cliver, 1994; Li et al., 2011; Thébault et al., 2010). Given that CHAOS-7 model estimates contribute three of the four geomagnetic sources (core, lithosphere, and magnetosphere) in MagGeo's framework, we can assume that MagGeo will capture long term changes in the geomagnetic field so long as the CHAOS-7 data inputs are updated. Models capture temporal changes related to secular variation, which arises from changes in the geomagnetic field over a few years due to the motion in the Earth's liquid outer core as well as the slow solar cycle variation of the magnetospheric field (Campbell, 2003).

Currently, we are using the CHAOS-7 model estimates (Finlay et al., 2020) but MagGeo's algorithm allows for integration of any other geomagnetic data sources within the VirES platform and may be modified as per the user's need. Specifically, the next couple years of high geomagnetic activity might be of interest to researchers studying the impact of geomagnetic activity on animal behavior. High geomagnetic activity events present a natural occurrence of an experimental extreme that could answer fundamental questions about animal behavior outside of laboratory settings through new "laboratories-in-the-wild" experimental approaches (Nathan et al., 2022). For all above scenarios, the MagGeo tool can facilitate exploration of these research questions.

5. Conclusion

With its relatively low error and flexible framework, MagGeo is a promising tool for movement ecologists and biologists who want to test animal navigation hypotheses about geomagnetism using open, high spatiotemporal resolution geomagnetic datasets. In addition to highlighting the strengths of MagGeo, our study also showcases the importance of error and accuracy tests for environmental covariate data that can be attached to animal movement data. As access to remotely sensed environmental data increases, it will be imperative to enlist cross-discipline expertise to maximize a dataset's full potential and understand the respective strengths and weaknesses of different datasets. Further, our research highlights the need for continued development of analytical tools for combining animal tracking with environmental data. As a research community, we can continue to learn how to better integrate multiple data sources to understand how an animal interacts with its environment thereby contributing to better protections of resources and its inevitable ties to the living world.

6. Funding Sources

This work was supported by funding from the Leverhulme Trust (Research Project Grant RPG-2018-258) and the Natural Sciences & Engineering Research Council of Canada

7. References

Åkesson, S., & Bianco, G. (2016). Assessing vector navigation in long-distance migrating birds. *Behavioral Ecology*, *27*(3), 865–875. https://doi.org/10.1093/beheco/arv231

Åkesson, S., & Bianco, G. (2017). Route simulations, compass mechanisms and long-distance migration flights in birds. *Journal of Comparative Physiology A*, *203*(6–7), 475–490. https://doi.org/10.1007/s00359-017-1171-y

Åkesson, S., Morin, J., Muheim, R., & Ottosson, U. (2005). Dramatic orientation shift of white-crowned sparrows displaced across longitudes in the high arctic. *Current Biology*, *15*(17), 1591–1597. https://doi.org/10.1016/j.cub.2005.07.027

Alerstam, T. (1987). Bird Migration Across a Strong Magnetic Anomaly. *Journal of Experimental Biology*, *130*(1), 63–86. https://doi.org/10.1242/JEB.130.1.63

Babayev, E. S., Hashimov, A. M., Yusifbeyli, N. A., Rasulov, Z. G., & Asgarov, A. B. (2006). Geomagnetic Storm Risks to Electric Power Distribution and Supply Systems at Mid-Latitude Locations and Their Vulnerability from Space Weather. *Technical and Physical Problems in Power Engineering*, 1097–1104.

Bartoń, K. (2022). *MuMIn: Multi-Model Inference: model selection and model averaging based on information criteria*. https://cran.r-project.org/package=MuMIn

Bates, D. M. (2010). Models With Multiple Random-effects Terms. In *lme4: Mixed-effects modeling with R* (1st ed., Vol. 1, pp. 27–54). Springer. https://lme4.r-forge.r-project.org/book/Ch2.pdf

Beason, R. C., & Semm, P. (1987). Magnetic responses of the trigeminal nerve system of the bobolink (Dolichonyx oryzivorus). *Neuroscience Letters*, *80*(2), 229–234. https://doi.org/10.1016/0304-3940(87)90659-8

Beggan, C. (2022). Evidence-based uncertainty estimates for the International Geomagnetic Reference Field. *Earth, Planets and Space*, *74*(1), 1–11. https://doi.org/10.1186/s40623-022-01572-y

Beggan, C., Macmillan, S., Hamilton, B., & Thomson, A. W. P. (2013). Independent validation of Swarm Level 2 magnetic field products and “Quick Look” for Level 1b data. *Earth, Planets and Space*, *65*(11), 1345–1353. https://doi.org/10.5047/eps.2013.08.004

Benitez-Paez, F., Brum-Bastos, V. da S., Beggan, C., Long, J. A., & Demšar, U. (2021). Fusion of wildlife tracking and satellite geomagnetic data for the study of animal migration. *Movement Ecology*, *9*(1), 1–19. https://doi.org/10.1186/S40462-021-00268-4

Benitez, F., & Long, J. (2022). *MagGeo/MagGeo-Annotation-Program: MagGeo*. Zenodo. https://doi.org/10.5281/ZENODO.6323249

Bianco, G., Ilieva, M., & Akesson, S. (2019). Magnetic storms disrupt nocturnal migratory activity in songbirds. *Biology Letters*, *15*(3), 20180918. https://doi.org/10.1098/rsbl.2018.0918

Boström, J. E., Åkesson, S., & Alerstam, T. (2012). Where on earth can animals use a geomagnetic bi-coordinate map for navigation? *Ecography*, *35*(11), 1039–1047. https://doi.org/10.1111/j.1600-0587.2012.07507.x

Brum-Bastos, V., Łoś, M., Long, J. A., Nelson, T., & Demšar, U. (2021). Context-aware movement analysis in ecology: a systematic review. *International Journal of Geographical Information Science*, 1–23. https://doi.org/10.1080/13658816.2021.1962528

Campbell, W. H. (2003). Introduction to Geomagnetic Fields. In *Introduction to Geomagnetic Fields* (2nd ed.). Cambridge University Press. https://doi.org/10.1017/cbo9781139165136

Carlson, B. S., Rotics, S., Nathan, R., Wikelski, M., & Jetz, W. (2021). Individual environmental niches in mobile organisms. *Nature Communications 2021 12:1*, *12*(1), 1–10. https://doi.org/10.1038/s41467-021-24826-x

Chernetsov, N., Pakhomov, A., Kobylkov, D., Kishkinev, D., Holland, R. A., & Mouritsen, H. (2017). Migratory Eurasian Reed Warblers Can Use Magnetic Declination to Solve the Longitude Problem. *Current Biology*, *27*(17), 2647-2651.e2. https://doi.org/10.1016/j.cub.2017.07.024

Chulliat, A., Macmillan, S., Alken, P., Beggan, C., Nair, M., Hamilton, B., Woods, A., Ridley, V., Maus, S., Thomson, A., House, M., Chulliat, A., Macmillan, S., Alken, P., Beggan, C., Nair, M., Hamilton, B., Woods, A., Ridley, V., … Thomson, A. (2015). *The US/UK World Magnetic Model for 2015-2020*. https://doi.org/10.7289/V5TB14V7

Cliver, E. W. (1994). Solar activity and geomagnetic storms: The first 40 years. *Eos, Transactions American Geophysical Union*, *75*(49), 569–575. https://doi.org/10.1029/94EO02041

Dodge, S., Bohrer, G., Weinzierl, R., Davidson, S. C., Kays, R., Douglas, D., Cruz, S., Han, J., Brandes, D., & Wikelski, M. (2013). The environmental-data automated track annotation (Env-DATA) system: linking animal tracks with environmental data. *Movement Ecology*, *1*(3), 1–14. https://doi.org/10.1186/2051-3933-1-3

European Space Agency. (2020). *SWARM*. https://earth.esa.int/web/guest/missions/esaoperational- eo-missions/swarm

European Space Agency. (2021). *VirES for Swarm*. https://vires.services/

Finlay, C. C., Kloss, C., Olsen, N., Hammer, M. D., Tøffner-Clausen, L., Grayver, A., & Kuvshinov, A. (2020). The CHAOS-7 geomagnetic field model and observed changes in the South Atlantic Anomaly. *Earth, Planets and Space*, *72*(1), 156. https://doi.org/10.1186/s40623-020-01252-9

Friis-Christensen, E., Lühr, H., & Hulot, G. (2006). Swarm: A constellation to study the Earth's magnetic field. *Earth, Planets and Space*, *58*(4), 351–358. https://doi.org/10.1186/BF03351933

Friis-Christensen, E., Lühr, H., Knudsen, D., & Haagmans, R. (2008). Swarm-An Earth Observation Mission investigating Geospace. *Advances in Space Research*, *41*(1), 210–216. https://doi.org/10.1016/j.asr.2006.10.008

Girdler, R. W., Taylor, P. T., Frawley, J. J., Girdler, R. W., Taylor, P. T., & Frawley, J. J. (1992). A possible impact origin for the Bangui magnetic anomaly (Central Africa). *Tectonophysics.*, *212*(1), 45–58. https://doi.org/10.1016/0040-1951(92)90139-W

Guilford, T., Åkesson, S., Gagliardo, A., Holland, R. A., Mouritsen, H., Muheim, R., Wiltschko, R., Wiltschko, W., & Bingman, V. P. (2011). Migratory navigation in birds: New opportunities in an era of fast-developing tracking technology. *Journal of Experimental Biology*, *214*(22), 3705–3712. https://doi.org/10.1242/jeb.051292

Hapgood, M. (2012). Prepare for the coming space weather storm. *Nature*, *484*(7394), 311–313. https://doi.org/10.1038/484311a

Holland, R. A., Thorup, K., Gagliardo, A., Bisson, I. A., Knecht, E., Mizrahi, D., & Wikelski, M. (2009). Testing the role of sensory systems in the migratory heading of a songbird. *Journal of Experimental Biology*, *212*(24), 4065–4071. https://doi.org/10.1242/jeb.034504

Hulot, G., Finlay, C. C., Constable, C. G., Olsen, N., & Mandea, M. (2010). The magnetic field of planet earth. *Space Science Reviews*, *152*(1–4), 159–222. https://doi.org/10.1007/s11214-010-9644-0

INTERMAGNET. (2020). *International Real-time Magnetic Observatory Network*. https://www.intermagnet.org/

Johnston, M. J. S. (1989). Review of magnetic and electric field effects near active faults and volcanoes in the U.S.A. *Physics of the Earth and Planetary Interiors*, *57*(1–2), 47–63. https://doi.org/10.1016/0031-9201(89)90213-6

Kakad, B., Kumar, R., & Kakad, A. (2020). Randomness in Sunspot Number: A Clue to Predict Solar Cycle 25. *Solar Physics*, *295*(6), 1–17. https://doi.org/10.1007/s11207-020-01655-7

Kays, R., Davidson, S. C., Berger, M., Bohrer, G., Fiedler, W., Flack, A., Hirt, J., Hahn, C., Gauggel, D., Russell, B., Kölzsch, A., Lohr, A., Partecke, J., Quetting, M., Safi, K., Scharf, A., Schneider, G., Lang, I., Schaeuffelhut, F., … Wikelski, M. (2022). The Movebank system for studying global animal movement and demography. *Methods in Ecology and Evolution*, *13*(2), 419–431. https://doi.org/10.1111/2041-210X.13767

Kerridge, D. (2001, December). INTERMAGNET: Worldwide near-real-time geomagnetic observatory data. *Proceedings of the Workshop on Space Weather*. https://www.intermagnet.org/publications/IM_ESTEC.pdf

Kikuchi, T. (2003). Space weather hazards to communication satellites and the space weather forecast system. *21st International Communications Satellite Systems Conference and Exhibit*, 2254. https://doi.org/10.2514/6.2003-2254

Kishkinev, D. (2015). Sensory mechanisms of long-distance navigation in birds: a recent advance in the context of previous studies. *Journal of Ornithology* , *156*(1), 145–161. https://doi.org/10.1007/s10336-015-1215-4

Kishkinev, D., Chernetsov, N., Pakhomov, A., Heyers, D., & Mouritsen, H. (2015). Eurasian reed warblers compensate for virtual magnetic displacement. *Current Biology*, *25*(19), R822–R824. https://doi.org/10.1016/j.cub.2015.08.012

Kloss, C. (2021). *ancklo/ChaosMagPy: ChaosMagPy v0.7*. https://doi.org/10.5281/ZENODO.5163844

Komolkin, A. V, Kupriyanov, P., Chudin, A., Bojarinova, J., Kavokin, K., & Chernetsov, N. (2017). Theoretically possible spatial accuracy of geomagnetic maps used by migrating animals. *Journal of the Royal Society Interface*, *14*(128), 20161002. https://doi.org/10.1098/rsif.2016.1002

Kranstauber, B., Cameron, A., Weinzerl, R., Fountain, T., Tilak, S., Wikelski, M., & Kays, R. (2011). The Movebank data model for animal tracking. *Environmental Modelling & Software*, *26*, 834–835. https://doi.org/10.1016/j.envsoft.2010.12.005

Krylov, V. V. (2017). Biological effects related to geomagnetic activity and possible mechanisms. *Bioelectromagnetics*, *38*(7), 497–510. https://doi.org/10.1002/bem.22062

Lanza, R., & Meloni, A. (2006). The earth's magnetism: An introduction for geologists. In *Springer Berlin Heidelberg*. Springer Berlin Heidelberg. https://doi.org/10.1007/978-3-540-27980-8

Lesur, V., Hamoudi, M., Choi, Y., Dyment, J., & Thébault, E. (2016). Building the second version of the World Digital Magnetic Anomaly Map (WDMAM). *Earth, Planets and Space*, *68*(1), 1–13. https://doi.org/10.1186/s40623-016-0404-6

Li, K. J., Feng, W., Liang, H. F., Zhan, L. S., & Gao, P. X. (2011). A brief review on the presentation of cycle 24, the first integrated solar cycle in the new millennium. *Ann. Geophys*, *29*, 341–348. https://doi.org/10.5194/angeo-29-341-2011

Lohmann, K. J., Lohmann, C. M. F., & Putman, N. F. (2007). Magnetic maps in animals: Nature's GPS. *Journal of Experimental Biology*, *210*(21), 3697–3705. https://doi.org/10.1242/jeb.001313

Lohmann, K. J., Putman, N. F., & Lohmann, C. M. F. (2008). Geomagnetic imprinting: A unifying hypothesis of long-distance natal homing in salmon and sea turtles. *Proceedings of the National Academy of Sciences of the United States of America*, *105*(49), 19096–19101. https://doi.org/10.1073/pnas.0801859105

Macmillan, S., & Olsen, N. (2013). Observatory data and the Swarm mission. *Earth, Planets and Space*, *65*(11), 1355–1362. https://doi.org/10.5047/eps.2013.07.011

Matzka, J., Chulliat, A., Mandea, M., Finlay, C. C., & Qamili, E. (2010). Geomagnetic observations for main field studies: From ground to space. *Space Science Reviews*, *155*(1–4), 29–64. https://doi.org/10.1007/s11214-010-9693-4

Mouritsen, H. (2014). Magnetoreception in Birds and Its Use for Long-Distance Migration. In *Sturkie's Avian Physiology: Sixth Edition* (pp. 113–133). Elsevier Inc. https://doi.org/10.1016/B978-0-12-407160-5.00008-7

Mouritsen, H. (2018). Long-distance navigation and magnetoreception in migratory animals. *Nature*, *558*(7708), 50–59. https://doi.org/10.1038/s41586-018-0176-1

Mouritsen, H., & Heyers, D. (2016). The Neural Basis of Long-Distance Navigation in Birds. *Annual Review of Physiology*, *78*(133–54), 610. https://doi.org/10.1146/annurev-physiol-

021115-105054

Muheim, R., Schmaljohann, H., & Alerstam, T. (2018). Feasibility of sun and magnetic compass mechanisms in avian long-distance migration. *Movement Ecology*, *6*(1), 1–16. https://doi.org/10.1186/s40462-018-0126-4

Naisbett-Jones, L. C., Putman, N. F., Stephenson, J. F., Ladak, S., & Young, K. A. (2017). A Magnetic Map Leads Juvenile European Eels to the Gulf Stream. *Current Biology*, *27*(8), 1236–1240. https://doi.org/10.1016/j.cub.2017.03.015

Nakagawa, S., & Schielzeth, H. (2013). A general and simple method for obtaining R2 from generalized linear mixed-effects models. *Methods in Ecology and Evolution*, *4*(2), 133–142. https://doi.org/10.1111/j.2041-210x.2012.00261.x

Nathan, R., Monk, C. T., Arlinghaus, R., Adam, T., Alós, J., Assaf, M., Baktoft, H., Beardsworth, C. E., Bertram, M. G., Bijleveld, A. I., Brodin, T., Brooks, J. L., Campos-Candela, A., Cooke, S. J., Gjelland, K., Gupte, P. R., Harel, R., Hellström, G., Jeltsch, F., … Jarić, I. (2022). Big-data approaches lead to an increased understanding of the ecology of animal movement. *Science*, *375*(6582), eabg1780. https://doi.org/10.1126/science.abg1780

Olsen, N., Friis-Christensen, E., Floberghagen, R., Alken, P., Beggan, C., Chulliat, A., Doornbos, E., Da Encarnação, J. T., Hamilton, B., Hulot, G., Van Den Ijssel, J., Kuvshinov, A., Lesur, V., Lühr, H., Macmillan, S., Maus, S., Noja, M., Olsen, P. E. H., Park, J., … Visser, P. N. (2013). The Swarm satellite constellation application and research facility (SCARF) and Swarm data products. *Earth, Planets and Space*, *65*(11), 1189–1200. https://doi.org/10.5047/eps.2013.07.001

Olsen, N., Hulot, G., & Sabaka, T. J. (2010). Measuring the earth's magnetic field from space: Concepts of past, present and future missions. *Space Science Reviews*, *155*(1–4), 65–93. https://doi.org/10.1007/s11214-010-9676-5

Olsen, N., Lühr, H., Sabaka, T. J., Mandea, M., Rother, M., Tøffner-Clausen, L., & Choi, S. (2006). CHAOS - A model of the Earth's magnetic field derived from CHAMP, Ørsted, and SAC-C magnetic satellite data. *Geophysical Journal International*, *166*(1), 67–75. https://doi.org/10.1111/j.1365-246X.2006.02959.x

Pettorelli, N., Laurance, W. F., O'Brien, T. G., Wegmann, M., Nagendra, H., & Turner, W. (2014). Satellite remote sensing for applied ecologists: opportunities and challenges. *Journal of Applied Ecology*, *51*(4), 839–848. https://doi.org/10.1111/1365-2664.12261

Pollonara, E., Luschi, P., Guilford, T., Wikelski, M., Bonadonna, F., & Gagliardo, A. (2015). Olfaction and topography, but not magnetic cues, control navigation in a pelagic seabird: Displacements with shearwaters in the Mediterranean Sea. *Scientific Reports*, *5*(1), 1–10. https://doi.org/10.1038/srep16486

Ridley, V., & Macmillan, S. (2014). *Validation of SWARM satellite magnetic data using observatory measurements*. http://nora.nerc.ac.uk/id/eprint/507837/1/Ridley_ValidationofSwarm.pdf

Sabaka, T. J., Tøffner-Clausen, L., Olsen, N., & Finlay, C. C. (2020). CM6: a comprehensive geomagnetic field model derived from both CHAMP and Swarm satellite observations.

Earth, Planets and Space, *72*(1), 1–24. https://doi.org/10.1186/s40623-020-01210-5

Schwarze, S., Steenken, F., Thiele, N., Kobylkov, D., Lefeldt, N., Dreyer, D., Schneider, N. L., & Mouritsen, H. (2016). Migratory blackcaps can use their magnetic compass at 5 degrees inclination, but are completely random at 0 degrees inclination. *Scientific Reports*, *6*(1), 1–10. https://doi.org/10.1038/srep33805

Semm, P., & Beason, R. C. (1990). Responses to small magnetic variations by the trigeminal system of the bobolink. *Brain Research Bulletin*, *25*(5), 735–740. https://doi.org/10.1016/0361-9230(90)90051-Z

Smith, A. (2020). *ESA-VirES/VirES-Python-Client: v0.6.2*. https://doi.org/10.5281/ZENODO.3872905

Sokolovskis, K., Bianco, G., Willemoes, M., Solovyeva, D., Bensch, S., & Åkesson, S. (2018). Ten grams and 13,000km on the wing - route choice in willow warblers Phylloscopus trochilus yakutensis migrating from Far East Russia to East Africa. *Movement Ecology*, *6*(1), 1–10. https://doi.org/10.1186/s40462-018-0138-0

Space Weather Live. (2021). *Solar Cycle 25 - Top 50 geomagnetic storms* . https://www.spaceweatherlive.com/en/auroral-activity/top-50-geomagnetic-storms/solar-cycle/25.html

St-Louis, B. (2012). *INTERMAGNET technical reference manual*. https://www.intermagnet.org/publications/intermag_4-6.pdf

Thébault, E., Purucker, M., Whaler, K. A., Langlais, B., & Sabaka, T. J. (2010). The magnetic field of the earth's lithosphere. *Space Science Reviews*, *155*(1–4), 95–127. https://doi.org/10.1007/s11214-010-9667-6

Walker, M., & Jackson, A. (2000). Robust modelling of the Earth's magnetic field. *Geophysical Journal International*, *143*(3), 799–808. https://doi.org/10.1046/j.1365-246X.2000.00274.x

Wikelski, M., Arriero, E., Gagliardo, A., Holland, R. A., Huttunen, M. J., Juvaste, R., Mueller, I., Tertitski, G., Thorup, K., Wild, M., Alanko, M., Bairlein, F., Cherenkov, A., Cameron, A., Flatz, R., Hannila, J., Hüppop, O., Kangasniemi, M., Kranstauber, B., … Wistbacka, R. (2015). True navigation in migrating gulls requires intact olfactory nerves. *Scientific Reports*, *5*(1), 1–11. https://doi.org/10.1038/srep17061

Wilcove, D. S., & Wikelski, M. (2008). Going, Going, Gone: Is Animal Migration Disappearing. *PLOS Biology*, *6*(7), e188. https://doi.org/10.1371/JOURNAL.PBIO.0060188

Wiltschko, R., & Wiltschko, W. (2013). The magnetite-based receptors in the beak of birds and their role in avian navigation. *Journal of Comparative Physiology A*, *199*(2), 89–98. https://doi.org/10.1007/s00359-012-0769-3

Wiltschko, R., & Wiltschko, W. (2021). The discovery of the use of magnetic navigational information. *Journal of Comparative Physiology A*, 1–10. https://doi.org/10.1007/s00359-021-01507-0

Wynn, J., Padget, O., Mouritsen, H., Perrins, C., & Guilford, T. (2020). Natal imprinting to the Earth's magnetic field in a pelagic seabird. *Current Biology*, *30*(14), 2869-2873.e2.

https://doi.org/10.1016/j.cub.2020.05.039

Zein, B., Long, J. A., Safi, K., Kölzsch, A., Benitez-Paez, F., Wikelski, M., Kruckenberg, H., & Demšar, U. (2022). Simulating geomagnetic bird navigation using novel high-resolution geomagnetic data. *Ecological Informatics*, 101689. https://doi.org/10.1016/j.ecoinf.2022.101689

Zein, B., Long, J. A., Safi, K., Kölzsch, A., Wikelski, M., Kruckenberg, H., & Demšar, U. (2021). Simulation experiment to test strategies of geomagnetic navigation during long-distance bird migration. *Movement Ecology*, *9*(1), 1–15. https://doi.org/10.1186/s40462-021-00283-5